

SCALING THE RESPONSE OF DELTAS TO RELATIVE SEA LEVEL CYCLES BY
AUTOGENIC SPACE AND TIME SCALES: A LABORATORY STUDY


AN ABSTRACT .

SUBMITTED ON THE 15th DAY OF MARCH 2017
TO THE DEPARTMENT OF EARTH AND ENVIRONMENTAL SCIENCES
IN PARTIAL FULFILLMENT OF THE REQUIREMENTS
OF THE SCHOOL OF SCIENCE AND ENGINEERING
OF TULANE UNIVERSITY
FOR THE DEGREE OF
MASTER OF SCIENCE


BY

Lizhu Yu


APPROVED:



Kyle M. Straub, Ph.D., Director



Nancye H. Dawers, Ph.D.



Nicole M. Gasparini, Ph.D

ABSTRACT

Relative Sea Level (RSL) change influences surface processes and stratigraphic architecture of deltaic systems and has been studied extensively for decades. However, we still lack a quantitative framework to define for a given delta what constitutes a small vs. large or short vs. long RSL cycle. We explore these questions with a suite of physical experiments that shared identical forcing conditions with the exception of sea level. We utilize two non-dimensional numbers that characterize the magnitude and period of RSL cycles. Magnitude is defined with respect to the maximum autogenic channel depth, while the period is defined with respect to the time required to deposit one channel depth of sediment, on average, everywhere in the basin. The experiments include: 1) a control experiment lacking RSL cycles, used to define autogenic scales, 2) a low magnitude, long period (LMLP) stage, and 3) a high magnitude, short period (HMSP) stage. We observe clear differences in the response of deltas to the forcing in each experiment. The RSL cycles in the HMSP stage induce allogenic surface processes and stratigraphic products with scales that exceed the stochastic variability found in the control stage. These include the generation of rough shorelines and large temporal gaps in the stratigraphy. In contrast, the imprint of LMLP cycles on surface processes and stratigraphy is found in properties that define the mean state of a system. These include the mean shoreline location and extraction of sediment inboard of the mean shoreline. This work demonstrates the effectiveness of defining RSL cycle magnitude and period through autogenic scales and

provides insights for generation of forward stratigraphic models influenced by RSL change.

SCALING THE RESPONSE OF DELTAS TO RELATIVE SEA LEVEL CYCLES BY
AUTOGENIC SPACE AND TIME SCALES: A LABORATORY STUDY

A THESIS

SUBMITTED ON THE 15th DAY OF MARCH 2017

TO THE DEPARTMENT OF EARTH AND ENVIRONMENTAL SCIENCES

IN PARTIAL FULFILLMENT OF THE REQUIREMENTS

OF THE SCHOOL OF SCIENCE AND ENGINEERING

OF TULANE UNIVERSITY

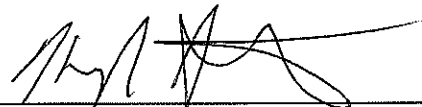
FOR THE DEGREE OF

MASTER OF SCIENCE

BY

Lizhu Yu

APPROVED:



Kyle M. Straub, Ph.D., Director



Nancye H. Dawers, Ph.D.



Nicole M. Gasparini, Ph.D

©Copyright by Lizhu Yu, 2017

All Rights Reserved

ACKNOWLEDGEMENT

Having the opportunity to study at Tulane with Professor Kyle Straub is one of the most rewarding and challenging things that I have done in my life. When I first came to Tulane, everything was so fresh to me. As time passed, I learned so many things through both academic and extracurricular time. I really appreciate all Kyle's help and patience through the past years. When I met difficulties and barriers in classes or research, his support and encouragement can always inspired me to fight against my fears and concerns. His passion and persistence for scientific research established the best model for me to further explore the scientific world. Meanwhile I also want to thank my committee members Professor Nancy Dawers and Professor Nicole Gasparini. They were always being supportive and approachable, and willing to help me out and give me guidance using their expertise.

Next I want to express my sincere thanks to the financial resources as that supported this work: National Science Foundation (grant EAR-1424312), a graduate student research grant from the Geological Society of America, and a summer research award from Schlumberger. I also want to thank the Department of Earth and Environmental Sciences for providing me the great opportunity to study at Tulane University.

I would also like to extend my special appreciation to the late Professor Paul Heller, who led me into this fabulous geological world. His guidance and strong support through my whole undergraduate time made me determined to continue learning the beauty of Earthscience, and gave me this opportunity to pursue my Master's Degree with Professor Kyle Straub at Tulane.

I also want to thank my family for all their continuous support and love. Words cannot describe how thankful I am to have them in my life. Thanks Chen Gui for all his love and undoubted support. I am so lucky to have him always stand by my side without any hesitation. I furthermore want to say thank you to Mengyuan Zheng, Yitong Luo, Xiangya Xu, Songlin Cai, Lian Zhang, Ziyao Li, Meng Xiong, Yingying Zhang, Yuan Li, Minming Cui, and every friend of mine who are always with me, and lend me a hand whenever I need.

Last but not least, I would not be able to stand at this point without tremendous help from our lab folks. I would like to express my great thanks to Dr. Qi Li, Christopher Esposito, Diana Di Leonardo, Tushar Bishnoi, Dr. Anjali Fernandes, Meg Harlan, Matthew Benson, and Stephan Toby. The bonding and power of the teamwork in our lab is the most meaningful thing that I will take with me forever.

TABLE OF CONTENTS

ACKNOWLEDGEMENT	ii
TABLE OF CONTENTS	iv
LIST OF FIGURES	v
Chapter 1: INTRODUCTION.....	1
Chapter 2: THEORY	6
Chapter 4: RESULTS.....	12
4.1.1 <i>Shoreline Response to RSL Cycles</i>	12
4.1.2 <i>Wetted Terrestrial Delta Fraction</i>	15
4.1.3 <i>System Mobility</i>	17
4.2 Stratigraphy.....	19
4.2.1 <i>Mass extraction</i>	19
4.2.2 <i>Stratigraphic architecture</i>	20
4.2.3 <i>Stratigraphic completeness</i>	24
5.1 Flow confinement and system mobility	26
5.2 Stratigraphic architecture	28
Chapter 6: DISCUSSION.....	30
6.1 Signal storage in the HMSP vs. LMLP stages	30
6.2 Large and/or long RSL cycles in field scale systems	35
Chapter 7: SUMMARY	38
FIGURES.....	40
REFERENCES.....	55
BIOGRAPHY	59

LIST OF FIGURES

- Figure 1:** Schematic of experimental setup and maps illustrating types of data collected over the course of each experimental stage.
- Figure 2:** Sea level cycles imposed for each experimental stage.
- Figure 3:** Overhead images of the three experimental stages.
- Figure 4:** Definition sketch of key variables and parameters used in the shoreline analysis.
- Figure 5:** Data defining the measured response of shorelines to changes in RSL.
- Figure 6:** Data defining the mean response of shorelines to changes in one cycle of RSL.
- Figure 7:** Data defining average response of the wetted fraction of the terrestrial delta-top to changes in RSL.
- Figure 8:** Data defining how the average fraction of a geomorphic surface modified by erosion or deposition varies from proximal to distal basin locations.
- Figure 9:** Data defining the measured response of deposit volume inboard of the average shoreline to changes in RSL.
- Figure 10:** Images of preserved physical stratigraphy of the three experimental stages.
- Figure 11:** Sand fraction measured from images of physical stratigraphy.
- Figure 12:** Panels of synthetic stratigraphy for a dip transect originating at the basin inlet colored by environment of deposition.
- Figure 13:** Panels of synthetic stratigraphy with deposits painted as a function of time of deposition within a cycle of RSL.

Figure 14: Stratigraphic completeness vs. time scale of discretization for the three experimental stages, measured from synthetic stratigraphy.

Figure 15: Predictions of magnitude and period of RSL cycles when normalized by autogenic length and time scales for 13 major river systems.

Chapter 1: INTRODUCTION

The influence of a receiving basin's water surface elevation, either lake or ocean level and commonly referred to as base level, on deltaic systems and their stratigraphic records is one of the most studied questions in all of geology. Going back to the work of Gilbert (1890), a plethora of studies tackled this question using observations made from field (Anderson, 2004; Bhattacharya, 2011; Blum and Tornqvist, 2000; Vail et al., 1977; Van Wagoner et al., 1990), numerical experiments (Burgess and Prince, 2015; Flemings and Grotzinger, 1996; Granjeon, 1999; Karssenberg and Bridge, 2008), and laboratory experiments (Heller et al., 2001; Koss et al., 1994; Li et al., 2016; Martin et al., 2009; Van Heijst and Postma, 2001). This body of work has led to an entire branch of stratigraphy termed sequence stratigraphy (Vail et al., 1977; Van Wagoner et al., 1990). While much is now known about the influence of sea level on deltas, we still lack a quantitative framework to define how the magnitude and period of base level cycles influence deltaic dynamics and their stratigraphic products for systems of various scales. Here we take a first pass at defining a normalized magnitude and period of base level cycles, in relation to the spatial and temporal scales of a delta's internal dynamics. Our goal is to link these normalized variables to characteristic morphodynamic and stratigraphic attributes in an effort to improve forward stratigraphic prediction and inversion of the stratigraphic record.

Following the early work of researchers like Gilbert (1890), Barrell (1917), and Wheeler (1964), Exxon's research lab during the 1970's made fundamental advances in our understanding of the influence of base level on stratigraphic architecture (Vail et al., 1977). Using two-dimensional seismic lines to characterize sedimentary packages along dip transects of continental margins, Vail et al. (1977) linked the timing of large scale changes in stratigraphic architecture to cycles of eustasy with magnitudes in excess of one hundred meters and periods in excess of one million years. Many recognize this work as the birth of sequence stratigraphy.

Building on the work of Vail et al. (1977), some researchers recognized similar stratigraphic patterns in continental margin stratigraphy, but at much finer scales. For example, using observations from outcrops exposed in the Book Cliffs of Utah, Van Wagoner et al. (1995) inferred changes in ocean elevation of the Great Interior Seaway with time scales of tens of thousands to hundreds of thousands of years and magnitudes of tens of meters. These interpretations were made from deposits of Cretaceous age, a time period known for greenhouse Earth conditions characterized by relatively small magnitude sea level fluctuations (Miller et al., 2005). More recent studies have sought to identify the stratigraphic signature of base level fluctuations with even shorter periods and of lower magnitudes. These include reevaluation of outcrop deposits in the Book Cliffs (Famubode and Bhattacharya, 2016), and numerical models that examine millennial scale base level cycles with magnitudes of twenty meters or less (Csato et al., 2014).

In their seminal work on clastic sequence architecture, Van Wagoner et al. (1990) define a hierarchy of scales for stacking patterns. Some of these scales, for example

lamina and beds, are discussed as products of a system's internal dynamics. On the other end of the spectrum, some scales are purely associated with external forcings. In the middle of their hierarchy, though, are deposits referred to as parasequences, which form over hundreds to tens of thousands of years and have thicknesses between meters to hundreds of meters. Van Wagoner et al. (1990) state that these could be the product of both internal dynamics and external forcings. However, when discussing specific deposits of this scale, Van Wagoner et al. (1990) and authors that follow their general methodology and nomenclature (Catuneanu, 2002; Hunt and Tucker, 1992; Plint, 2009) often do not consider a system's internal dynamics, but prefer arguments based on external drivers, such as base level.

While early work on deltaic stratigraphy focused on external forcings, the last ten years has seen an explosion in the number of studies that focus on the internal dynamics of deltaic systems and their stratigraphic products (Hickson et al., 2005; Karamitopoulos et al., 2014; Kim et al., 2006; Li et al., 2016; Van Dijk et al., 2009; Wang et al., 2011). This has largely been led by results coming from experimentalists working with deltas produced in laboratory settings. The reason behind this is simple: experimental deltas with horizontal scales of meters constructed over tens to hundreds of hours allow researchers to directly observe a system's internal dynamics. Examples of these internal dynamics include bar migration, avulsions, and deltaic lobe switching. Physical experiments also allow researchers to explore the influence of boundary and forcing conditions, as these can be accurately controlled in laboratory settings. Observations from these experiments suggest that internal deltaic dynamics, often referred to as autogenics, can influence surface dynamics and stratigraphic records over much greater time scales

than previously thought: tens of thousands to hundreds of thousands of years (Kim and Paola, 2007; Kim et al., 2006; Wang et al., 2011). Motivated by these experimental observations, several recent studies used numerical experiments to isolate the influence of autogenic processes and support the influence of autogenics on stratigraphy out to time scales important to basin filling (Dalman et al., 2015; Liang et al., 2016). These physical and numerical experiments are starting to produce a reevaluation of field scale stratigraphic architecture that incorporates autogenics in their interpretations (Chamberlin and Hajek, 2015; Hajek et al., 2012; Hofmann et al., 2011).

Physical experiments have been used to study the influence of base level cycles on stratigraphic architecture for some time now (Heller et al., 2001; Koss et al., 1994; Li et al., 2016; Martin et al., 2009; Van Heijst and Postma, 2001; Wood et al., 1993). Here we highlight work by Heller et al (2001) which examined the influence of “short” and “long” base level cycles. In this study, performed in the eXperimental Earth-Scape (XES) basin, short and long were in reference to the equilibrium channel response time, T_{eq} , of the system to an external forcing. T_{eq} is defined by Paola et al. (1992) as the time associated with a basin evolving to the condition where subsidence and sedimentation are balanced, which scales as:

$$T_{eq} \cong \frac{L^2}{\nu} \quad (1)$$

where L is the characteristic length of a system and ν is a transport (diffusion) coefficient. Heller et al (2001) found that when a base level cycle was long in comparison to T_{eq} , systems tend to generate laterally extensive unconformities without the formation of incised valleys, whereas the inverse is true for base level cycles that are short with respect

to T_{eq} . While this study examined “short” and “long” base level cycles, they did not examine the influence of the magnitude of a base level cycle.

Recently, Li et al. (2016) examined the influence of both cycle magnitude and period on the storage of base level information in stratigraphy. In their study, Li et al. (2016) define storage thresholds associated with the space and time scales of a system’s autogenic processes. This allowed them to define cycle magnitude and period for systems of varying size through a comparison of the scale of the external forcing to the scale of the internal dynamics. The main thrust of the work of Li et al. was an examination of deposition rate time series with the aim of defining storage thresholds for base level changes in stratigraphy.

The goal of this thesis is to more fully characterize the surface processes and stratigraphic attributes associated with base level cycles that are stored either due to their large magnitude or long period. Specifically, we hypothesize 1) that base level cycles with large magnitudes but short periods will be characterized by allogenic surface processes and stratigraphic products with scales that exceed the stochastic variability found in unforced systems; and 2) base level cycles with long periods but small magnitudes will generate detectable changes in the mean characteristics of the stratigraphy, e.g. mean deposition rates, deposit grain sizes and/or mean location of paleo-shoreline indicators, from those in an unforced system.

Chapter 2: THEORY

Here we present theory to define the magnitude and period of Relative Sea Level (RSL) cycles through a comparison of the scales of deltaic autogenic processes. Here RSL change is defined as the sum of local absolute sea level rise and subsidence rates. Our definitions follow those proposed by Li et al. (2016) and are represented here for completeness and clarity.

Starting with the magnitude of RSL cycles: we compare the range of a RSL cycle, M_{RSL} , (i.e. difference in elevation from cycle peak to trough) to the depth of the largest channels, H_c , that are observed in a system with constant boundary conditions:

$$H^* = \frac{M_{RSL}}{H_c} \quad (2).$$

We use H_c because the largest autogenic elevation changes are associated with post avulsion channel incision. Next we compare the period of a RSL cycle, T_{RSL} , to the maximum time scale of autogenics in deltaic systems. Wang et al. (2011) defined this as the compensation time scale, T_c , and showed that it scaled with the time necessary to deposit, on average, one channel depth of stratigraphy everywhere in a basin. In other words, T_c , represents the time necessary for a particle deposited at Earth's surface to be buried to a depth that is no longer susceptible to remobilization from autogenic incision events (Straub and Esposito, 2013). This produces a non-dimensional time that scales as:

$$T^* = \frac{T_{RSL}}{T_c} \quad (3).$$

Combined, H^* and T^* provide a method with which to compare a normalized magnitude and period of RSL cycles to the morphodynamics of individual systems.

Chapter 3: EXPERIMENTAL METHODS

To study the influence of RSL cycles on surface processes and stratigraphic records we conduct a series of physical laboratory experiments. As outlined in a review by Paola et al. (2009), physical experiments produce spatial structure and kinematics that, although imperfect, compare well with natural systems despite differences of spatial scale, time scale, material properties, and number of active processes. As a result, these experiments provide morphodynamic and stratigraphic insight into the evolution of channelized settings under an array of external and internal influences.

Experiments were conducted in the Delta Basin at the Tulane University Sediment Dynamics and Stratigraphy Laboratory. This basin is 4.2 m long, 2.8 m wide, and 0.65 m deep (Fig. 1). Ocean level is controlled through a weir, which is in hydraulic communication with the basin. The weir is on a computer controlled vertical slide that allows for sub-millimeter scale ocean elevation control. The ocean elevation was monitored and logged once a minute with a transducer to ensure that its elevation matched target elevations. Water and sediment supply are also controlled through this computer interface and were kept at constant values of $1.7 \times 10^{-4} \text{ m}^3/\text{s}$ and $3.9 \times 10^{-4} \text{ kg/s}$, respectively for each experiment.

We first performed a control experiment, TDB-12, with constant forcing conditions to define the autogenic time and space scales necessary to calculate H^* and T^* . These forcings include a constant rate of sea level rise (or pseudo-subsidence) with a rate, \bar{r} , equal to 0.25 mm/hr, that resulted in a near constant terrestrial accommodation

production rate that matched the volumetric input rate of sediment to the experiment. As a result, the mean location of the shoreline only varied due to autogenic processes during the course of the experiment. This experiment was run for 900 hrs and resulted in a deposit thickness of approximately 225 mm. The input sediment mixture was designed to mimic earlier experimental work (Hoyal and Sheets, 2009) and had particles' diameter ranging from 1 to 1000 μm with a mean of 67 μm and was dominantly quartz that was white in color. One quarter of the coarsest 23.5% of the distribution was commercially dyed to aid visualization of stratigraphic architecture. A small amount of commercially available polymer (New Drill Plus distributed by Baker Hughes Inc.) was added to the sediment mixture to enhance sediment cohesion. In all experiments discussed, the input water to the basin was dyed with a food coloring to aid characterization of morphodynamics. From this experiment we were able to define H_c as 12.25 mm and T_c as 49 hr.

Next we performed experiment TDB-15-1, designed to isolate the influence of cycle magnitude and period on deltaic morphodynamics and stratigraphy. TDB-15-1 had identical forcing conditions to those detailed for TDB-12, with the exception of RSL cycles that varied in magnitude and period. The shape of the RSL cycles were defined by a sine wave, which is a simplification of Milinkovic cycles whose shape depends on a number of climatic and paleo-geographic parameters (Miller et al., 2005). The first stage of TDB-15-1 had RSL cycles defined by $H^* = 0.5$ and $T^* = 2$, while the second stage had RSL cycles defined by $H^* = 2.0$ and $T^* = 0.5$ (Fig. 2). We will refer to the first stage as the Low Magnitude Long Period (LMLP) stage and the second stage as the High Magnitude Short Period (HMSP) stage. Li et al. (2016) showed that systems with values

of H^* or T^* much greater than one are associated with stratigraphic RSL signal storage. As such the first experimental stage will highlight storage due to RSL period and the second stage will highlight storage due to RSL magnitude. In each stage RSL cycled for 490 run-hours, producing approximately 120 mm of stratigraphy per stage.

Data was collected during the course of each experiment to define system morphodynamics and stratigraphy. Starting with system morphodynamics, a digital camera mounted directly above the basin collected photographs of the active delta top every 15 minutes. These images are used to analyze the evolving flow field of each experiment (Fig. 3).

Next, a FARO Focus3D-S 120 laser scanner was used to monitor the topography in each experiment. This instrument captures an elevation point cloud that can be converted into digital elevation models (DEMs) with horizontal grid spacing of 5 mm in the down and cross basin directions and with a vertical resolution of approximately 1 mm. DEMs cover an arc defined by a radius of 1.3 m from the entrance to the basin. This was generally either delta top or upper delta foreset for the majority of the experiment. The laser scanner also houses a digital camera such that each point is tagged with an RGB color value. One scan was taken near the end of each run hour with the flow on, while a second scan was collected at the end of each run hour with the flow turned off. These color-coded digital elevation models can be used for both morphodynamic and stratigraphic analysis. The co-registered DEMs and digital images allow the flow field to be directly tied to topography, which aids morphodynamic analysis. For stratigraphic analysis, the topography can be used to construct synthetic stratigraphic volumes. This is done by stacking all topographic scans and clipping scans for erosion.

Finally, at the end of each experiment we sectioned the deltas along cross-sectional transects at 0.76 m and 1.22 m from the basin infeed point. This was done by inserting a metal wedge into the deposit after the water level in the basin was raised to an elevation that flooded the entire deposit. The metal wedge was then filled with dry ice and methanol which resulted in a chemical reaction that lowered the temperature of the wedge to a value sufficient to freeze the pore water in the deposit and the surrounding deposit to the wedge. The wedge was then extracted from the basin providing a view of the preserved stratigraphy which was then photographed with digital cameras.

Chapter 4: RESULTS

In this section we present results that characterize the influence of RSL cycle magnitude and period on deltaic morphodynamics and the resulting stratigraphy. We are particularly interested in comparing these morphodynamics and stratigraphic products to those produced in systems with constant forcings. As such, results from each analysis will include a comparison to our control experiment with constant forcings. We start by characterizing the surface dynamics in each experiment, as we have far more data to quantify these dynamics compared to the resulting three-dimensional stratigraphic architecture. We focus, however, on dynamics that are closely tied to depositional processes. We then characterize the stratigraphy of each experiment utilizing stacked topographic scans clipped for erosion (synthetic stratigraphy) coupled to our limited number of physical stratigraphy images.

4.1 Morphodynamics

4.1.1 Shoreline Response to RSL Cycles

We start our characterization of RSL influence on morphodynamics by quantifying shoreline dynamics in each experimental stage. We are interested in how RSL cycles influence both the mean location and rate of movement of the shoreline in addition to the variability of these parameters. Our interest in shoreline dynamics stems from the importance of this boundary in separating terrestrial and marine processes, and

because channels are prone to deposition when reaching the shoreline. As such the shoreline strongly influences both surface processes and the stratigraphy.

Using the DEMs and measured time series of sea level, we identify a line that defines the shoreline each run-hour. The distance from the basin entrance to the shoreline, $s_{i,j}$, was then calculated for all points that define this line, where i is an index that refers to each spatial measurement of distance to the shoreline and j is an index that refers to the run-hour (Fig. 4A). We use these measurements of $s_{i,j}$ to calculate the mean distance to the shoreline for each run-hour (\bar{s}_j) and the mean distance to the shoreline for an entire stage (\bar{s}_{st}). This is done for the control experiment, as well as the LMLP and HMSP experimental stages. Starting with the control experiment, we observe differences in \bar{s}_j relative to \bar{s}_{st} with magnitudes up to 0.14 m (Fig. 5B). As expected, in both the LMLP and HMSP stages the position of \bar{s}_j is out of phase with RSL (i.e. high RSL corresponds to short \bar{s}_j). The amplitude of changes to \bar{s}_j in the stages with RSL cycles are larger than autogenic changes observed in the control experiment. Next, we characterize the mean response of \bar{s}_j to one full cycle of RSL by averaging the response of \bar{s}_j for each cycle in stages with RSL cycles (5 cycles in the LMLP stage and 20 cycles in the HMSP stage); (Fig. 6). To generate a similar plot for the control experiment, we average sequential segments of the control experiment that have duration equal to one T_c , starting from the beginning of the control stage. While both stages with RSL cycles show a response of \bar{s}_j that is near completely out of phase with RSL, the magnitude of this response was two times greater in the HMSP stage compared to the LMLP stage.

Motivated by an analysis of shoreline movement in the earlier discussed XES experiments (Kim et al., 2006), we are interested in defining the influence of RSL on the rate of shoreline movement and the variability in this rate. To do this we track the position of the shoreline each run-hour along nine transects that each originate at the basin entrance and are separated by an angle of $\pi/8$ (Fig. 4B). We then calculate the rate of shoreline movement along each transect for sequential run hours. This allows us to calculate the mean rate of shoreline movement during a given run-hour ($\dot{\bar{s}}_j$) (Fig. 5C) and the standard deviation of this rate $\sigma(\dot{s}_j)$ (Fig. 5D). Similar to our analysis of \bar{s}_j we average all cycles for a given stage to see the mean response of $\dot{\bar{s}}_j$ and $\sigma(\dot{s}_j)$ to RSL (Fig. 6C&D). We observe a clear response of $\dot{\bar{s}}_j$ and $\sigma(\dot{s}_j)$ to RSL in the HMSP stage with $\dot{\bar{s}}_j$ being approximately $1/4$ out of phase with RSL and $\sigma(\dot{s}_j)$ being in phase with RSL. Observations for the LMLP stage are less clear. A muted signal of $\dot{\bar{s}}_j$ is observed while $\sigma(\dot{s}_j)$ shows no response above the autogenic perturbations.

Our next morphodynamic analysis is focused on the roughness of the shoreline (R_{SL}). We define R_{SL} as:

$$R_{SL} = \sqrt{\frac{1}{N} \sum_{i=1}^N \left(\frac{s_{i,j} - \bar{s}_j}{\bar{s}_j} \right)^2} \quad (4)$$

where N is the total number of measurements that define the shoreline at run-hour j (Fig. 5E and Fig. 6E). In both the HMSP and LMLP stages we observe changes in R_{SL} that are in phase with RSL. However, the response of R_{SL} to RSL is much stronger in the HMSP experiment compared to the LMLP experiment.

We note that all metrics used to define the shoreline and its movement show stronger responses in the HMSP stage compared to the LMLP stage. In fact, some of the metrics ($\dot{\bar{s}}_j$ and R_{SL}) show barely detectable signals in the LMLP stage while no detectable signal is found for $\sigma(\dot{s}_j)$.

4.1.2 Wetted Terrestrial Delta Fraction

Next, we characterize the influence of RSL cycles on the fraction of the terrestrial deltaic surface covered by active flow. This is motivated by observations and theory that predict channel incision and flow confinement in valleys during periods of falling and low base level, while periods of rising and high base level are linked to channel backfilling and loss of confinement (Heller et al., 2001; Karssenberg and Bridge, 2008; Van Wagoner et al., 1990). This suggests that the fraction of the terrestrial surface covered by flow should decrease as flow is confined in deep incisional channels during base level fall, and that this fraction should rise as confinement is lost during base level rise as flow becomes laterally distributed. Observations of the active deltaic surface suggest that changes in flow confinement are linked to position within a RSL cycle (Fig. 3). To measure this in our experiments we start by using the topographic maps and imposed time series of sea level to extract all terrestrial delta pixels (elevation > sea level). Each terrestrial delta cell is converted to an area equal to $2.5 \times 10^{-5} \text{ m}^2$, determined by the geometry of the imposed topographic grid. This allows the total terrestrial area, A_{TD} , to be calculated for each run-hour. Next, we calculate the area of the terrestrial delta covered by flow, A_{wet} . Using the Red (R), Green (G), and Blue (B) color bands recorded

in the digital images collected by the scanner, we calculate the color intensity, I , of the terrestrial cells as:

$$I = \frac{B - G - R}{B + G + R} \quad (5a)$$

when the flow was dyed blue and as:

$$I = \frac{R - G - B}{B + G + R} \quad (5b)$$

when the flow was dyed red. A threshold intensity value is then set to separate wet from dry regions. This threshold was picked by identifying a value that on visual inspection appeared to accurately separate the two regions. Finally, the wetted fraction (f_w) of the terrestrial delta is calculated as:

$$f_w = \frac{A_{wet}}{A_{TD}} \quad (6).$$

Similar to attributes defining the morphodynamics of the shoreline in response to RSL cycles, we calculate a mean response of f_w to one full cycle of RSL by averaging the response of all cycles in a given experimental stage (Fig. 7).

In the LMLP and HMSP stages a similar response of f_w is observed, which is maximized during RSL highstand and minimized during RSL lowstand, consistent with existing theory (Catuneanu, 2002). However, the magnitude of the response and signal-to-noise ratio is greater in the HMSP relative to LMLP stage. A similar calculation for the mean f_w over a period equivalent to T_c in the control experiment shows no significant structure. The response of f_w for the stages with RSL cycles is in phase with RSL and we note that by analysis of Eq. 6 this response could occur by simply reducing A_{TD} through transgression during RSL rise with a constant proximal to distal increase in confinement.

However, we essentially always observed a proximal to distal decrease in flow confinement associated with distributary channel networks.

4.1.3 System Mobility

Existing theory suggests that the mobility of deltaic systems is minimized during periods of low RSL and maximized during periods of high RSL (Heller et al., 2001; Karssenberg and Bridge, 2008; Van Wagoner et al., 1990). Similar to f_w , the tie between RSL and system mobility is linked to the lateral confinement of flow in incised valleys during falling RSL and valley filling and associated high avulsion rates during rising and high RSL. As the generation of incised valleys and channel avulsion deposits are prominent stratigraphic features in deltaic stratigraphy, we are interested in characterizing the surface processes that generate them. Previous experimental studies characterized system mobility by quantifying the amount of time necessary for 95% of a delta-top to be visited by flow in overhead images of the transport system (Cazanacli et al., 2002; Kim et al., 2010; Straub and Esposito, 2013). Given the high temporal resolution of our topographic data we decide to take a different approach and measure a proxy of mobility by tracking the number of grid locations that experience significant geomorphic work over the course of a run-hour.

We refer to elevation changes, either erosion or deposition, as modifying or regrading the transport surface and as such define modification as a change in elevation of at least 1 mm, the vertical resolution of our DEMs. We track surface modification along circular transects defined by specified radii from the basin entrance. As such, these transects are roughly oriented perpendicular to the mean flow direction (Fig. 8A). This is

done for transects ranging from 0.35 m to either 1.2 m (the control stage) or 1.3 m (stages with RSL cycles) from the basin entrance, each separated by 0.05 m. For each transect and each run-hour, we measure the fraction of grid cells along a transect that experience surface modification, f_m . Similar to analysis presented above, the average f_m response to RSL is determined by calculating f_m for each run-hour and for each transect, and then averaging all measurements that share the same distance from the basin entrance and the same number of run-hours into a RSL cycle. This produces time-space maps of f_m , where time is presented as the fraction of time into a full cycle of RSL and distance is relative to the basin entrance (Fig. 8B-D). On each time-space map we also plot a line that represents the mean shoreline location to aid interpretation of trends.

From the time-space maps of surface modification we make the following observations: 1) The control stage shows the lowest fraction of surface modification of all of the stages and no consistent temporal trend over the course of a T_c cycle. 2) The LMLP stage shows a slightly higher fraction of surface modification, compared to the control experiment. This reworking shows only muted spatial and temporal trends, with modification minimized during periods of low RSL. 3) The HMSP stage shows clear spatial and temporal trends in modification compared to the other two stages. Locations on and just downstream of the mean shoreline show f_m values far in excess of those observed in the two other stages. In addition, during periods of low RSL f_m values upstream of the mean shoreline are extremely low, suggesting low system mobility. During rising RSL, locations upstream of the mean shoreline show f_m values higher than those measured at most locations in the control and LMLP stages.

4.2 Stratigraphy

In the following section we characterize the influence of RSL cycle magnitude and period on resulting stratigraphic deposits. Similar to our morphodynamic characterization, we compare the temporal and spatial scales of stratigraphic products in stages that experienced RSL cycles to both the mean and stochastic attributes of the stratigraphy from our control experiment.

4.2.1 Mass extraction

Our first stratigraphic analysis centers on the influence of RSL cycles for the storage of sediment in terrestrial and marine settings. The motivation is similar to the analysis of Li et al. (2016) who worked with this same set of experiments. In their study, Li et al. calculated the average deposition rate along strike oriented transects, for each hour of the three experimental stages. This was done at relatively proximal and distal locations on the experimental delta-tops. They found that when either RSL cycle magnitude or period exceeded the spatial or temporal scales of autogenic processes, the period of the RSL cycle was imbedded in the power spectral of the average deposition rates.

Whereas Li et al. focused on analysis of mean deposition rates along individual strike transects, our aim is to analyze the volumetric extraction of mass in settings that are dominantly terrestrial vs. dominantly marine. We start this analysis by generating a time series of the total volume of sediment stored inboard of the mean shoreline of both the control experiment and the experiment with RSL cycles (\bar{s}). We define this volume as $V_{s,inboard \bar{s}}$ (Fig. 9B). We focus on measuring the growth of the deposits inboard of this

mean shoreline because 1) we expect enhanced growth of this volume during periods of high RSL as channels meet a shoreline inboard of its mean position and 2) large water depths past the mean shoreline of any given stage resulted in frequent data outages and as such prevent us from characterizing this region. Coincidentally, the position of the mean shoreline in each stage occurred at a distance where approximately 48-51% of the mass input to the basin was extracted to deposition. As such, approximately half of the sediment was deposited in dominantly terrestrial settings and half in dominantly marine settings. While data outages prevent us from testing, our expectation is that the trend in volume growth past the mean shoreline is completely out of phase with the growth inboard of the mean shoreline.

In each experimental stage a long term growth of $V_{s,inboard \bar{s}}$ is observed, resulting from the long term generation of accommodation in the basin. We subtract this long term trend, estimated with a least-squares linear regression of the growth of $V_{s,inboard \bar{s}}$, to analyze the influence of RSL in perturbations of $V_{s,inboard \bar{s}}$ (Fig. 9C). Finally, similar to our analysis of morphodynamic attributes, we average the response of the detrended $V_{s,inboard \bar{s}}$ to each cycle to generate a mean response (Fig. 9D). In both the LMLP and HMSP stages we see a clear response of the detrended $V_{s,inboard \bar{s}}$ to RSL, with a phase shift of one quarter cycle and a response that is of similar magnitude in both stages with RSL cycles.

4.2.2 Stratigraphic architecture

While the volumetrics discussed above inform us about long term trends in mass extraction, we are also interested in the architecture of the stratigraphy resulting from

each experiment, including the geometry and grain size of stratigraphic sequences. We start our characterization of stratigraphic architecture with panels of physical stratigraphy imaged along proximal and distal strike transects (Fig. 10). In our control experiment we observe strata composed of coarse channel-fill deposits and fine-grained overbank deposits at the proximal transect. Prominent channel-levee deposits segregate the coarse channel body deposits from the fine overbank. The stratigraphy from the proximal transect of the experiment with RSL cycles also contains coarse channel-fill deposits and fine overbank zones, but lacks the well-developed levees found in the strata of the control experiment. While the stratigraphy of the LMLP and control stages share similar numbers of channel bodies, the strata of the HMSP stage contain slightly more channel bodies, with more frequent evidence of incision at their bases.

The stratigraphy of the distal strike transects are dominantly composed of coarse terminal channel lobe deposits and fine overbank and marine strata. The distal stratigraphy of the control experiment is markedly coarser than the strata of the stages with RSL cycles, with each coarse lobe deposit separated by thin fine grained strata that are relatively laterally continuous. In contrast the average size of lobe deposits is less in the LMLP stage relative to the control strata and further less in the strata of the HMSP stage. These differences in lobe sizes are associated with an increase in the volume of fine strata as the magnitude of RSL cycles increased from the control stage to the LMLP and finally to the HMSP stage.

We quantify the differences in coarse sand content in the strata of each stage at the proximal and distal transects by taking advantage of the commercially dyed coarse sediment and the dominantly white fine sediment. Similar to our analysis of the wetted

terrestrial delta-top fraction, we use the R, G, and B color bands of the physical stratigraphy images to calculate the color intensity of each pixel using Eq. 5 and utilize a threshold intensity value that through visual inspection appears to separate coarse from fine sediment. We then calculate the fraction of coarse colored sediment for the stratigraphy of each stage at each transect (Fig. 11). This allows us to make the following observations. For both the proximal and distal transects the stratigraphy of the HMSP stage is measurably finer than the strata of the LMLP and control stages. At the proximal transect the strata of the control and LMLP stages share similar sand fractions, while the control strata of the distal transect is markedly coarser than the LMLP stage strata. For each stage the strata is coarser at the distal compared to the proximal transect.

While the physical stratigraphy gives valuable information on the segregation of particles based on grain size, unfortunately we were only able to collect two strike sections per stage. In addition, while the architecture of the physical stratigraphy is influenced by RSL, defining environments and timing of deposition relative to RSL cycles based solely on the physical stratigraphy would require imprecise interpretations. To overcome these problems, we assemble volumes of synthetic stratigraphy, generated by stacking DEMs with topography clipped to account for sediment removed during erosional events (Martin et al., 2009). Knowledge of the run-time and sea level associated with each DEM allows us to paint this synthetic stratigraphy with attributes like depositional environment (terrestrial vs. marine) and the location within a RSL cycle when sediment at a particular location was deposited.

Using the co-registered sea level and DEMs, we separate portions of the stratigraphy deposited in terrestrial vs. marine settings. When viewed in dip panels, we

note prominent parasequences in the stratigraphy of the control stage that resulted from autogenic transgressions and regressions of the shoreline in conjunction with active deposition (Fig. 12A). These parasequences have length scales of up to 0.75 m and thicknesses are up to 13 mm. The parasequences in the LMLP and HMSP experiments show differences with the control experiment. These include flooding surfaces that extend upstream of those found in the control experiment. In addition, the thickness of the parasequences in the LMLP stage (Fig. 12B) exceeded those of the control stage, while parasequence thickness in the HMSP stage (Fig. 12C) never reached the thicknesses seen in the control stage.

Next, we paint the synthetic stratigraphy by the position within a RSL cycle in which sediment was deposited (Fig. 13). This process is done to test if the RSL cycles induce spatial trends in the location of RSL signal storage and to visualize the characteristic length scales of deposits associated with a RSL cycle in each stage. Again we wish to compare the stages with RSL cycles to our control stage, but this introduces a problem as our control experiment lacked RSL cycles. To overcome this we paint the control stratigraphy with a similar color map as the stages with RSL cycles, but with color defined by the position within sequential blocks of time of duration equal to T_c , starting at the beginning of the control stage. Here we compare stratigraphy in both dip (Fig. 13A-C) and strike sections from relatively proximal (Fig. 13D, F, H) to relatively distal (Fig. 13E,G,I) locations.

Starting with the stratigraphy viewed in dip, as expected there is no dominant upstream to downstream trend in the timing of deposition within a cycle of T_c in the control experiment. We also observe no dominant spatial trend in the timing of deposition

within a cycle of RSL in the LMLP stage. There is, however, a strong spatial trend in the HMSP stage dip stratigraphy. While stratigraphy from the basin entrance to approximately 0.7 m from the source shows no clear preference for position within a RSL cycle, from 0.7 to 1.2 m from the source deposition dominantly occurred during RSL highstands. Downstream of this zone deposition dominantly occurred during RSL lowstands.

In strike transects we observe similar trends to those seen in dip, with strata in the proximal transects of the HMSP stage constructed mainly of highstand deposition and distal strata constructed mainly of lowstand deposition. In addition, we note that the lateral continuity of the time of deposition, for both the proximal and distal transects of the LMLP stage, exceeds those of the control and HMSP stages.

4.2.3 Stratigraphic completeness

Our final analysis centers on the temporal completeness of the strata preserved in each experimental stage. Similar to previous studies (Sadler and Strauss, 1990; Straub and Esposito, 2013), we define stratigraphic completeness as the fraction of intervals, n , along vertical 1-D stratigraphic sections discretized at t , which leave a record in the form of preserved sediment over the length of a given section that has a total time, T :

$$C = \frac{nt}{T} \quad (7).$$

We are interested in the completeness of each stage as it helps define if stratigraphic sections have sufficient temporal coverage to extract the sequencing of paleo-surface processes and environmental forcings. We also focus on completeness of entire experimental stages as this provides adequate experimental run-time to sample the full

array of dynamics and products of each stage, rather than focusing for example on the completeness during one particular lowstand. As noted by Ager (1973) and quantified by Sadler and Strauss (1990) and Straub and Esposito (2013), stratigraphic completeness depends on the time interval at which a record is discretized, where completeness increases as t increases. Gaps in the stratigraphic record of systems with constant forcings occur due to periods of stasis on geomorphic surfaces and erosional events that occur due to stochastic autogenic channel dynamics. Processes resulting from allogenic forcings, like flooding of deltaic surfaces due to RSL rise, can also reduce stratigraphic completeness.

We quantify stratigraphic completeness by calculating the 1-D completeness of all grid nodes in a given stage and then averaging these values to get a representative value for the stage. We start by measuring completeness at the finest temporal resolution available to us in our experiments, that being with t set to 1 hr. We then analyze the effect of t on C . Using our synthetic stratigraphic volumes we proceed by systematically coarsening the temporal resolution of our synthetic stratigraphy from the initial measurement resolution to a final resolution equal to $0.5T$, for each stage, by Δt steps of 1 hr. Then for each value of t we apply Eq. 7 to calculate C . From the resulting plot of C as a function of t for each stage (Fig. 14) we make the following observations. 1) As t increases C increases for each stage until saturating at 100%. 2) Over short time scales the control stage has the highest completeness followed closely by the LMLP experiment, while the HMSP experiment consistently has the lowest completeness.

Chapter 5: INTERPRETATION

5.1 Flow confinement and system mobility

Measurements that define the average response of the terrestrial wetted fraction and surface modification to RSL cycles indicate influences on flow confinement and the mobility of transport systems. Starting with flow confinement: in both the LMLP and HMSP stages we observed a minimum in f_w during lowstands, while f_w was maximized during highstands (Fig. 7). We interpret the reduction of f_w during lowstands as indicating an increase in flow confinement. The stronger response in the HMSP stage is likely associated with the funneling of flow into net incisional channels during periods with high rates of base level fall. The low magnitude and long period of the sea level cycles in the LMLP stage, coupled with the long term pseudo-subsidence, meant that base level never actually decreased in the LMLP stage (Fig. 2). Periods of falling base level in the HMSP stage increased flow confinement as river capture resulted in fewer, but deeper channels that were more capable of incision.

It is worth noting that we did not observe wide-spread formation of incised valleys and resulting regional unconformities in our experiments. This is starkly different from previous experiments that used non-cohesive sediment mixtures and produced incised valleys that rapidly evolved through vertical incision and lateral erosion during periods of base level fall and rise (Heller et al., 2001; Martin et al., 2011). We note that some modern systems do possess strongly cohesive substrates (Stanley et al., 1996)

that would reduce incision and lateral erosion rates during base level fall. However, our experiments are likely more cohesive, relative to typical shear stresses on the experimental surfaces, than many field scale systems, while earlier experiments possibly sit at the other extreme end of the cohesion spectrum.

The confinement of flow during lowstands and loss of confinement during highstands also influenced the mobility of the transport systems. Our measurements indicate that the LMLP stage was only slightly more likely to experience topographic modifications at any time, compared to the control stage (Fig. 8). We take this observation as indication that the control and LMLP stages shared similar rates of system mobility. Exploration of time lapse videos of these stages also supports that they shared similar styles of system mobility, which was dominated by channel avulsion and rapid mobility during channel reorganization phases. In contrast, the fraction of the transport surface modified each hour was higher in the HMSP stage and this modification was strongly coupled to the position of the shoreline. We interpret this as a signal of lobe deposition as channels terminated in the ocean. During periods of high sea level, locations upstream of the shoreline had high surface modification values which when coupled to observations from time-lapse photography are interpreted as the product of frequent avulsions induced by rapid sea level rise rates which induced in-channel deposition. The opposite is observed in the HMSP stage during periods of falling sea level, when locations inboard of the shoreline had low surface modification values interpreted as a result of channel incision.

Finally, the interpreted increase in flow confinement and decrease in lateral mobility as the magnitude of RSL cycles increased is likely the reason why stratigraphic

completeness decreased as RSL magnitudes increased (Fig. 14). Flow confinement and reduction in lateral mobility would increase time-scales of stasis on geomorphic surfaces and aid incision during falling base level, both of which lead to time-gaps in stratigraphy.

5.2 Stratigraphic architecture

Panels of the physical stratigraphy displayed in figure 10 show significant differences between experimental stages and between the proximal to distal transects. Here, we interpret causes for some of the differences we detailed in the results section. We start with the observation that the control stage displays the most well-developed levee deposits. This is interpreted as the consequence of the constant forcings in this stage, which provided no external perturbations to destabilize the transport system. In contrast, the cycles of RSL in the other stages aided the destabilization of channels, specifically during rising RSL when in-channel deposition was maximized, leading to channel superelevation and the set-up conditions necessary for channel avulsion.

While some differences are observed in the proximal stratigraphy of the three stages, more pronounced differences are observed in the distal strata from the three stages. The distal strata from the control experiment is mainly composed of coarse terminal channel lobe deposits separated by thin, fine-grained, and laterally extensive deposits interpreted as condensed sections resulting from autogenic transgressions. These condensed sections are the result of the pumping of fine grained sediment to the marine, which was transported in suspension within the terrestrial channels. This resulted in plumes of fine sediment downstream of the shoreline and aided the construction of pro-delta deposits, in addition to the condensed sections within the deltaic stratigraphy. The

fraction of the strata composed of coarse sediment decreased in the LMLP stage and further still in the HMSP stage (Fig. 10). We interpret this as the result of more frequent flooding due to the allogenicly forced shoreline transgressions. Specifically, the high magnitude shoreline transgressions in the HMSP stage resulted in large volumes of fine sediment deposited in shallow water depths over the majority of the delta-top surface. Given the limited lateral mobility of channels during sea level fall, much of this fine-grained strata was preserved during falling sea level resulting in relatively small and coarse lobe deposits encased in thick fine grained sections. The shoreline transgressions in the HMSP stage extended upstream of the proximal transect location, likely enhancing deposition of fines there as well, which we interpret as the reason why the proximal HMSP strata is finer than the strata of the two other stages.

Chapter 6: DISCUSSION

6.1 Signal storage in the HMSP vs. LMLP stages

Analyses detailed in the results and interpretation sections focused on testing our two main hypotheses, which we return to here. The first hypothesis stated that RSL cycles with large magnitudes but short periods would result in surface processes and stratigraphic products with scales that exceed the stochastic variability found in unforced systems. Support for this hypothesis can be found in many of our morphodynamic and stratigraphic results. Starting with shoreline dynamics, we highlight that the shoreline in the HMSP stage was characterized by high migration rate variability that produced rougher shorelines than observed in either the control or LMLP stages (Fig. 5 & 6). This allogenic variability and roughness was maximized during periods of rapid RSL rise as channels on the delta-top delivered sediment to the shoreline, which helped counter the shoreline transgressions that occurred at other inactive locations of the delta-top. This observation is similar to findings in earlier experimental studies (Kim et al., 2006). In contrast, any allogenic variability in shoreline migration rates and roughness in the LMLP stage did not rise above the stochastic autogenic signal.

Further morphodynamic support for our first hypothesis can be found in the time-space maps of surface modification (Fig. 8). While the surface modification maps of the LMLP stage indicate only a slight increase in the fraction of modification per run-hour, compared to the control experiment, a clear and strong allogenic signal can be found in the HMSP maps. In the HMSP stage high fractions of surface modification were strongly

tied to the position of the shoreline with values that far exceeded the stochastic autogenic values of the control stage. The signal was not restricted to the shoreline, though. During periods of low RSL, surface modification fractions inboard of the shoreline were noticeably less than found in the control stage, while periods of high RSL were associated with surface modification fractions inboard of the shoreline that were noticeably higher than the control stage.

The allogenic surface dynamics discussed above resulted in stratigraphic attributes that also support our first hypothesis. The frequent and widespread flooding induced by the high magnitude RSL cycles of the HMSP stage, that were in excess of the autogenic transgressions in the control stage, decreased the fraction of sand stored in its stratigraphy relative to the other stages (Fig. 10&11). Interestingly, in at least one sense the short period of the RSL cycles in the HMSP stage resulted in deposit scales that were less than those found in the control stage. Here we refer to the thicknesses of parasequences (Fig. 12). In the control stage, parasequences had thicknesses up to the scale of the largest channels and formed over time scales comparable to T_c . As RSL cycled with a period that was half T_c in the HMSP stage, their allogenic parasequences had less time to develop and as such were approximately half as thick as the autogenic parasequences in the control stage. While the allogenic parasequences of the HMSP stage were thinner than the control stage, flooding surfaces in the HMSP stage did extend farther inboard of the mean shoreline than those of the control stage.

The last attribute of the stratigraphy that we wish to highlight in regard to our first hypothesis concerns stratigraphic completeness (Fig. 14). The allogenic increase in flow confinement and reduction in system mobility during falling RSL in the

HMSP stage increased periods of stasis on the geomorphic surface relative to the control stage. Enhanced incision during rapid falling of RSL in the HMSP stage also aided removal of sediment from the record. These two processes increased the number and duration of time gaps in the HMSP stage relative to either the control or LMLP stages. As such extraction of paleo-environmental records from HMSP influenced deltas will be fairly incomplete, relative to unforced or LMLP systems, at time scales short relative to T_c . However, all systems converge to 100% completeness at approximately T_c . When combined, we suggest that the data presented supports the notion that high magnitude RSL cycles result in allogenic surface processes and stratigraphic products that are generally higher in magnitude than the autogenic processes and products found in unforced systems.

We now turn our attention to our second major hypothesis, that RSL cycles with long periods but small magnitudes produce a response in attributes that define the mean state of a system. Here we highlight one morphodynamic and one stratigraphic attribute that we suggest support this hypothesis. The morphodynamic result focuses on the location of the mean shoreline (Fig. 6). While the RSL cycles in the LMLP stage did not induce high variability in the migration rate of the shoreline or cause enhanced shoreline roughness, a clear signal can be found in the shoreline position over the course of an average RSL cycle. As expected, the position of the mean shoreline in relation to the basin entrance is perfectly out of phase with the elevation of sea level during an RSL cycle.

Movement of the shoreline during the course of a RSL cycle in the LMLP stage also resulted in a clear stratigraphic signature. Here we refer to the extraction of sediment

to the deltaic stratigraphy inboard of the mean shoreline. Results presented in figure 9 indicate that transfer of mass to the deltaic stratigraphy inboard of the mean shoreline was enhanced during periods of high RSL. As a result, local maximum in volume stored inboard of the mean shoreline occurred at the falling inflection of RSL cycles as RSL proceeded below its mean value. A signal of this process in the LMLP stage is observed that is of equal or slightly higher magnitude as that observed in the HMSP stage (Fig. 9D). This result, when viewed in conjunction with our other analyses suggests that small magnitude but long period RSL cycles, as defined by autogenic time and space scales, do little to change the time scales of stochastic deltaic surface processes. However, their long period allows small differences in surface processes, for example the rate of sediment extraction, to compound and produce noticeable differences in the statistics of the final deposit. These results support our second hypothesis.

It is worth highlighting that the clear response of the mean shoreline (Fig. 5&6) and sediment extraction inboard of the mean shoreline (Fig. 9) observed in the LMLP stage is found after temporally averaging the influence of five RSL cycles. This averaging process results in response curves for the control experiment that lack structure, while aiding identification of the response in the LMLP experiment. However, it might be difficult to do this type of averaging for field systems unless stratigraphic age control is available that is linked to knowledge of the timing of RSL cycles. Prior to temporal averaging, identifying a signal in the raw time-series of sediment extraction inboard of the mean shoreline that differs in magnitude to the stochastic autogenic perturbations found in the control experiment is difficult. This result highlights the need

for better theory to define the scales of autogenic perturbations for field systems and further development of techniques to filter these perturbations from field datasets.

While the mass extraction signature of RSL cycles might require large amounts of chronostratigraphic data, our results on the scales of parasequences hint to possible facies signatures of both the LMLP and HMSP RSL cycles. The parasequences of the control experiment had maximum thicknesses that scaled with the depth of the largest autogenic channels and as previously noted by Straub et al. (2015) their maximum proximal to distal extent scaled with the system's backwater length, L_B . The backwater length approximates the distance upstream of the shoreline where channels start to feel the influence of their receiving basin and scales as:

$$L_B \approx \frac{H_C}{S} \quad (8)$$

(Chow, 1959), where S is the slope of the transport system. In both the LMLP and HMSP stages the maximum proximal to distal extent of the parasequences exceed L_B while parasequence thickness was much greater than H_C in the LMLP stage and much less than H_C in the HMSP stage. Estimation of channel depths through preserved channel bodies or complete bar forms (Mohrig et al., 2000; Paola and Borgman, 1991) and methods to estimate paleo-slopes (Lynds et al., 2014) provide means to estimate H_C and L_B for paleo systems. As a result, one could compare parasequence lateral extends and thicknesses to the autogenic H_C and L_B scales as a means of RSL cycle signal identification.

We close this section by noting that the manifestation of the RSL cycles in the HMSP stage is a change in the architecture of the resulting stratigraphy, including the scale of deposit packages. These architectural differences might be detectable with limited time control. However, with the exception of parasequence scales, the

manifestation of the RSL cycles in the LMLP experiment was found in more gradually varying parameters, like the extraction of mass from transport. These signals might require precise geochronological control to observe in field scale stratigraphy.

6.2 Large and/or long RSL cycles in field scale systems

Given our discussion of the morphodynamic and stratigraphic attributes of RSL cycles, when normalized by autogenic temporal and spatial scale, an obvious question is where and when might we expect to find either LMLP or HMSP systems. To address this, we use a database of modern systems where information concerning H_c and T_c were compiled. This database was first presented by Li et al. (2016) who visualized the information in a slightly different way than presented here. T_c was estimated for these systems using information compiled on the long term aggradation rates of systems and the relationship:

$$T_c = \frac{H_c}{\bar{r}} \quad (9)$$

(Wang et al., 2011). H_c and T_c are then compared to Milankovitch-scale RSL cycles in the middle Pleistocene to the present when eccentricity cycles (~100 k.y.) resulted in RSL changes of ~100 m and late Miocene conditions when obliquity cycles (~40 k.y.) resulted in RSL changes with ranges of 10–35 m. Similar to Li et al., we highlight that H_c values in our database are constructed from modern channel depths and we acknowledge that some change in channel depths have occurred since the late Miocene due to changing boundary conditions. However, these changes are unlikely to influence the general observations highlighted below. These comparisons are made quantitatively with Eqs. 2 & 3 and shown in figure 15. With this compilation we make the following observations.

Given the high magnitude of middle Pleistocene to present eccentricity cycles, all systems in our database for this time are characterized by H^* values in excess of one. Between the middle Pleistocene to present many of these systems are also characterized by high T^* values. Thus, some but not all systems in our database can be characterized as HMSP during the middle Pleistocene to present.

The decrease in amplitude of RSL cycles in the late Miocene reduces the H^* of systems in our database, but associated with this is a decrease in T^* as the late Miocene was dominated by shorter duration obliquity cycles. As a result, we again observe some HMSP and high magnitude long period systems during the late Miocene, but no systems that confidently fall within the LMLP quadrant. This leads to the question: do Milankovitch cycles ever lead to LMLP RSL deltaic systems? While not included in our database, several observations from literature suggest that this might be possible. Examination of Eqs. 2, 3, & 8 indicate that the following conditions are necessary to produce a LMLP RSL system. First, deep channels aid the ability to get low H^* values from small magnitude cycles. Second, basins with high subsidence rates help decrease T_c and thus help increase T^* .

Candidate systems which could fulfil the conditions outlined above include 1) the Frish Creek-Vallecito Basin filled by the paleo-Colorado River delta. Deltaic stratigraphy, imaged in outcrops from this basin and deposited 4-5 Ma, have dune cross bedding with scales up to 10 m (Dorsey, personal communication) which could indicate channel depths up to 30 m (Paola and Borgman, 1991). In addition, basin subsidence rates were exceptionally high with sustained rates up to 2.2 mm/yr (Dorsey et al., 2011).

These values and characteristic eustatic cycles during this time (Miller et al., 2005) suggest H^* and T^* values of approximately 0.5 and 2, respectively.

Additional LMLP candidate systems might exist in the Cretaceous stratigraphy of large river delta systems. The Cretaceous exemplifies greenhouse Earth conditions when limited or no continental scale glaciers existed, which reduced the magnitude of Milankovitch scale RSL cycles. Some studies suggest that RSL cycles were as long as 100 or 300 kyrs during this period (Haq, 2014). As a result, systems of a Mississippi River Delta scale or larger during this time might be characterized as LMLP. Again, we note that our results would suggest that stratigraphic evidence from these systems, that would indicate their forcing by LMLP RSL cycles, might necessitate high precision geochronology data.

Chapter 7: SUMMARY

The work detailed above builds on a long history of investigation into the influence of RSL cycles on deltaic surface processes and stratigraphic products. Here, we specifically build on the work of Li et al. (2016) who presented an approach to normalize the magnitude and period of RSL cycles by deltaic autogenic time and space scales. The goal of this manuscript was to thoroughly document how surface processes and stratigraphic products vary in experimental deltas that experience either high magnitude but short period or low magnitude but long period RSL cycles. Exploration of surface processes focused on those with clear links to the preserved stratigraphic record. The main results are summarized as follows:

1. Our analysis indicates that the response of deltas to HMSP RSL cycles can be found in morphodynamic processes with rates and scales that exceed the stochastic autogenic variability found in systems with constant forcings. These morphodynamics produce stratigraphic architecture with scales that are significantly different from autogenic stratigraphy and with lower stratigraphic completeness that results from the observed changes in surface dynamics. Specifically, we find that HMSP RSL cycles result in deltas with spatially variable shoreline migration rates that yield rough shorelines. These cycles induce significant reductions in system mobility during lowstands and enhance mobility during highstands. Their high magnitude aids retention of fines in delta-top stratigraphy and reduces the thickness of parasequences compared to autogenic

systems. Finally, their stratigraphy shows clear proximal to distal bands where timing of deposition is strongly dictated by position within the RSL cycle.

2. The morphodynamic and stratigraphic response to the LMLP cycles was more subtle. Stochastic attributes of the surface processes, for example variability in shoreline migration rates, were only slightly different from the control experiment. However, the long period of these cycles allowed small differences to sum together to give clear signals in attributes like the mean shoreline location or the mass extraction inboard of the mean shoreline. We suggest that the recognition of these types of cycles in field scale stratigraphy might be challenging due to limited architectural differences relative to constantly forced systems, but high precision geochronology might aid signal extraction.
3. Analysis of channel depths and long term sedimentation rates from 13 major river deltas suggest that Milankovitch eustatic sea level cycles during both the late Miocene and middle Pleistocene to present are frequently of high magnitude but short period compared to autogenic scales. While no RSL cycles during these times for the systems in our database could be characterized as low magnitude and long period some evidence from prior studies suggest that these types of cycles might have existed in the past.

FIGURES

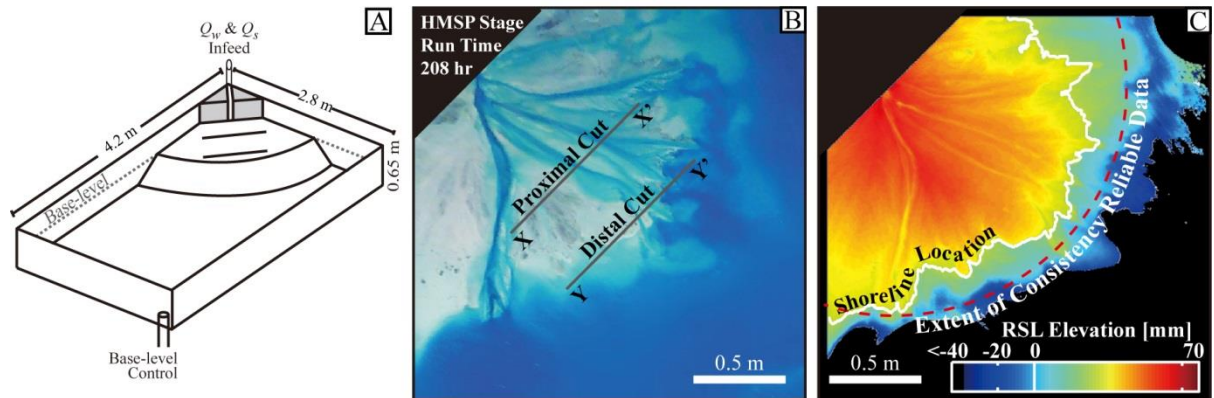


Figure 1: Schematic of experimental setup and maps illustrating types of data collected over the course of each experimental stage. A) Schematic diagram of Tulane Delta Basin with key basin dimensions and controls labeled. B) Characteristic digital image of the HMSF stage with flow on and dyed for visualization. Image collected with laser scanner such that all pixels are referenced relative to the basin coordinate system. Locations of physical stratigraphic sections are shown by solid black lines. C) DEM of experimental surface collected with laser scanner. Solid white line denotes shoreline. Dashed red line shows the extent of DEMs where topography was reliably measured for each run-hour.

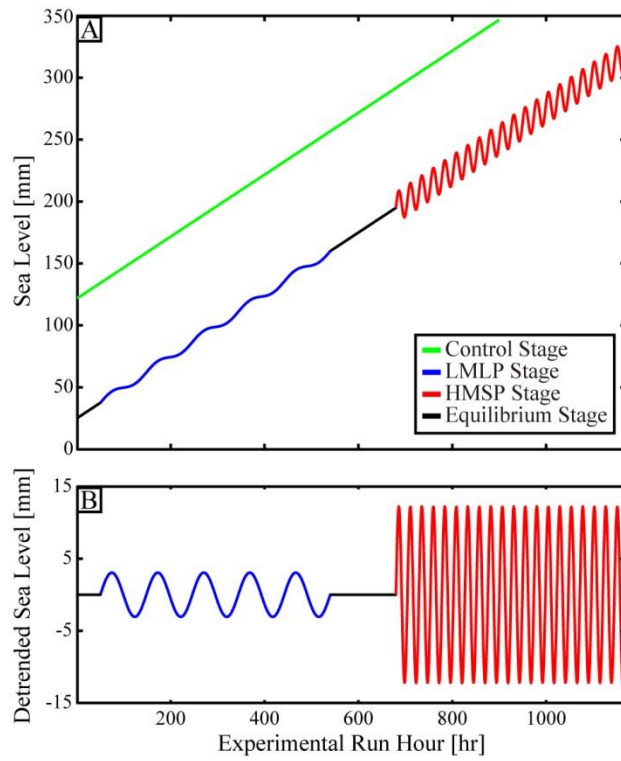


Figure 2. A) Sea level change over the course of the three experimental stages. B) History of sea level in each experimental stage after long-term trend has been removed.

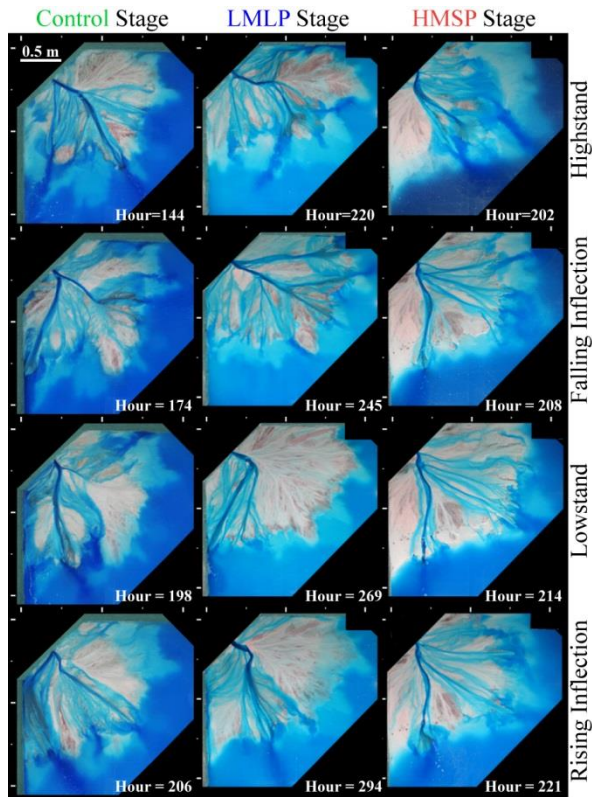


Figure 3: Overhead images of the three experimental stages. Images display system morphology at key points through a RSL cycle, or equivalent durations into a cycle of duration equal to T_c for the control stage.

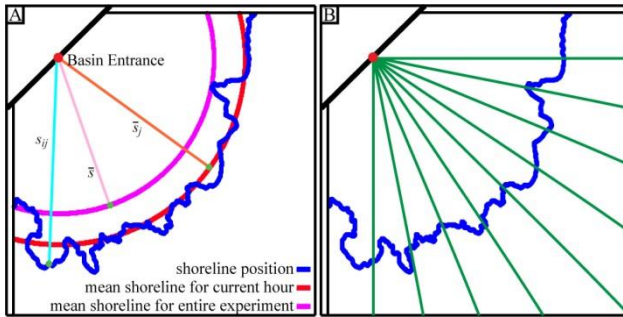


Figure 4: Definition sketch of key variables and parameters used in the shoreline analysis. A) sketch detailing shoreline position, mean shoreline position for a given run-hour, and mean shoreline position for an entire experiment. B) sketch detailing location of transects used in calculation of shoreline migration rate and variability of this rate.

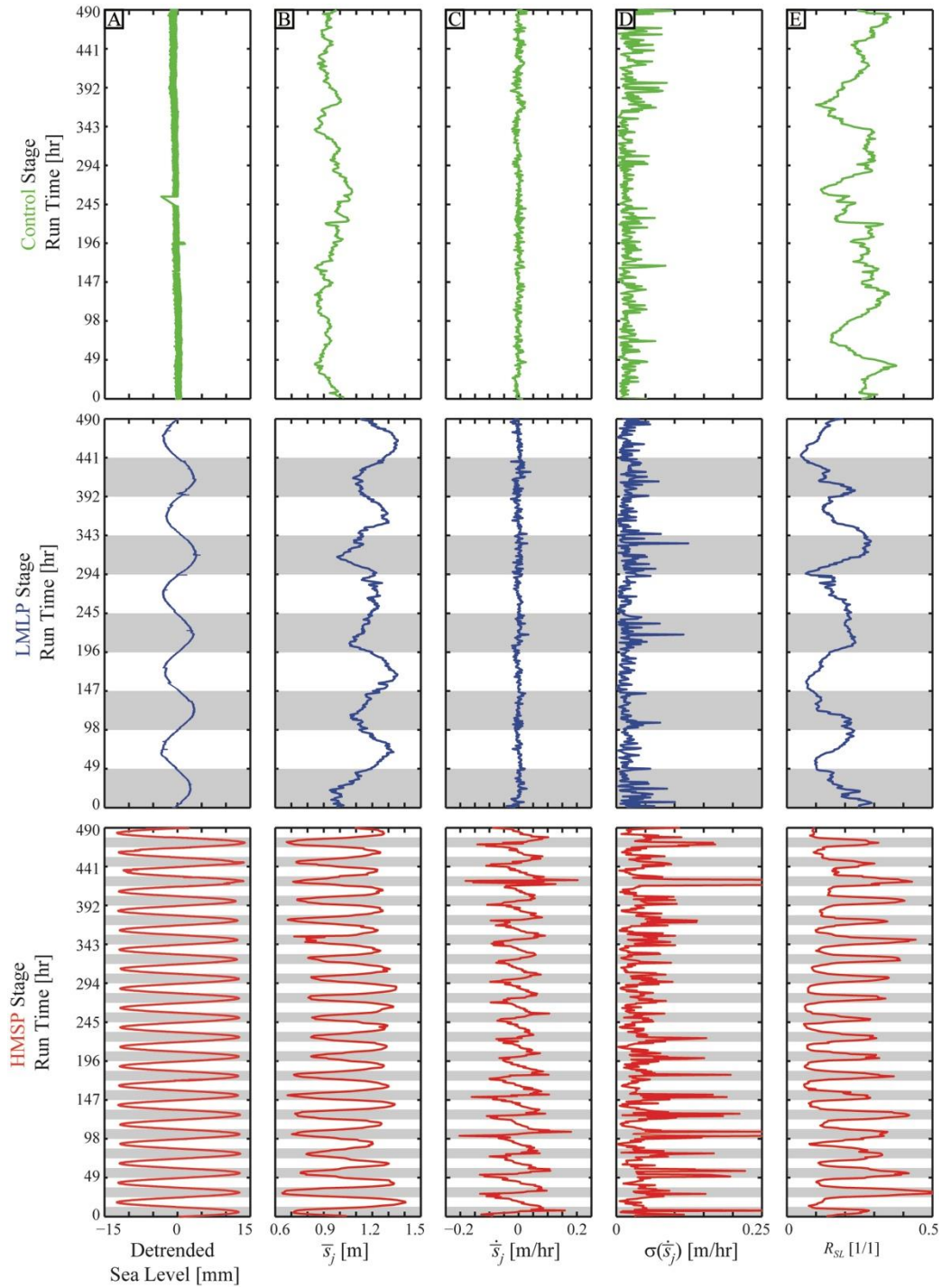


Figure 5: Data defining the measured response of shorelines to changes in RSL and the variability of this response. A) Time series of measured sea level detrended for long term sea level rise in each experimental stage. B) Time series of the mean distance from the basin entrance to the shoreline. C) Time series of the mean shoreline migration rate. Negative values indicate shoreline moving landward. D) Time series of the variability of the rate of shoreline migration. E) Time series of the shoreline roughness. Gray bars indicate periods when sea level was higher than average.

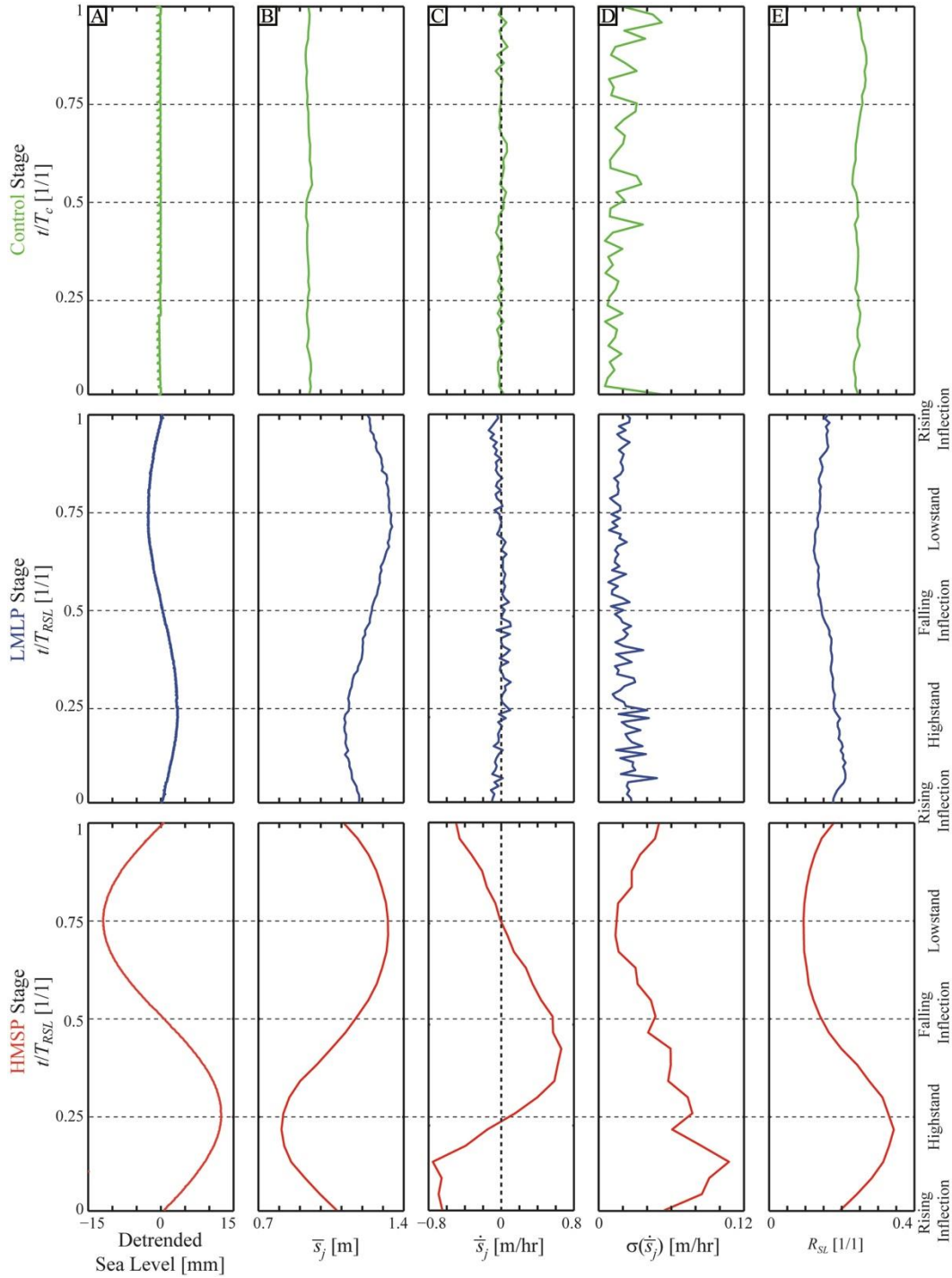


Figure 6: Data defining the mean response of shorelines to changes in an average cycle of RSL and the variability of this response. A) Average measured sea level detrended for long term sea level rise in each experimental stage. B) Average response of the mean distance from the basin entrance to the shoreline. C) Average response of the mean shoreline migration rate. Negative values indicate shoreline moving landward. D) Average response of the variability of the rate of shoreline migration. E) Average response of the shoreline roughness.

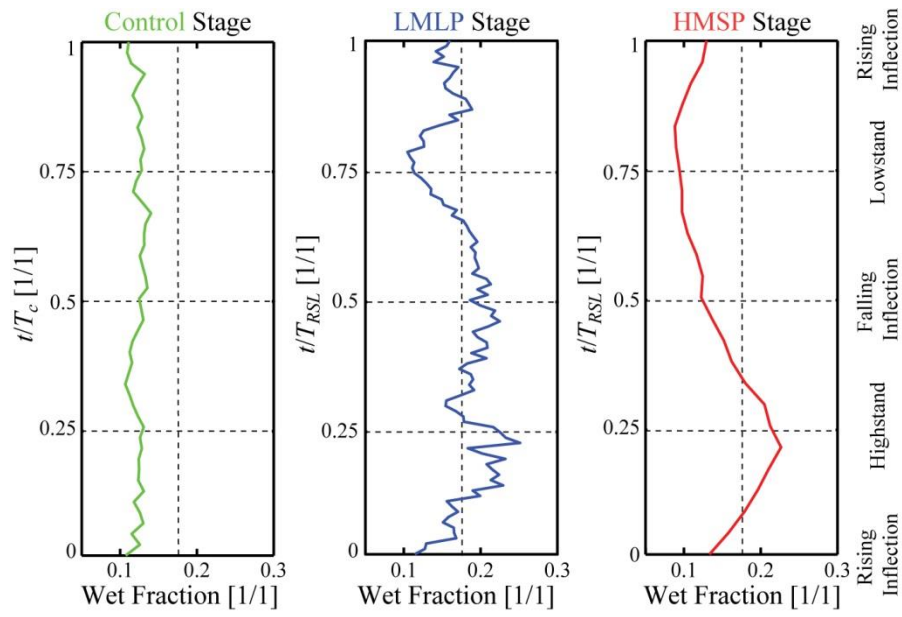


Figure 7: Data defining average response of the wetted fraction of the terrestrial delta-top to changes in RSL.

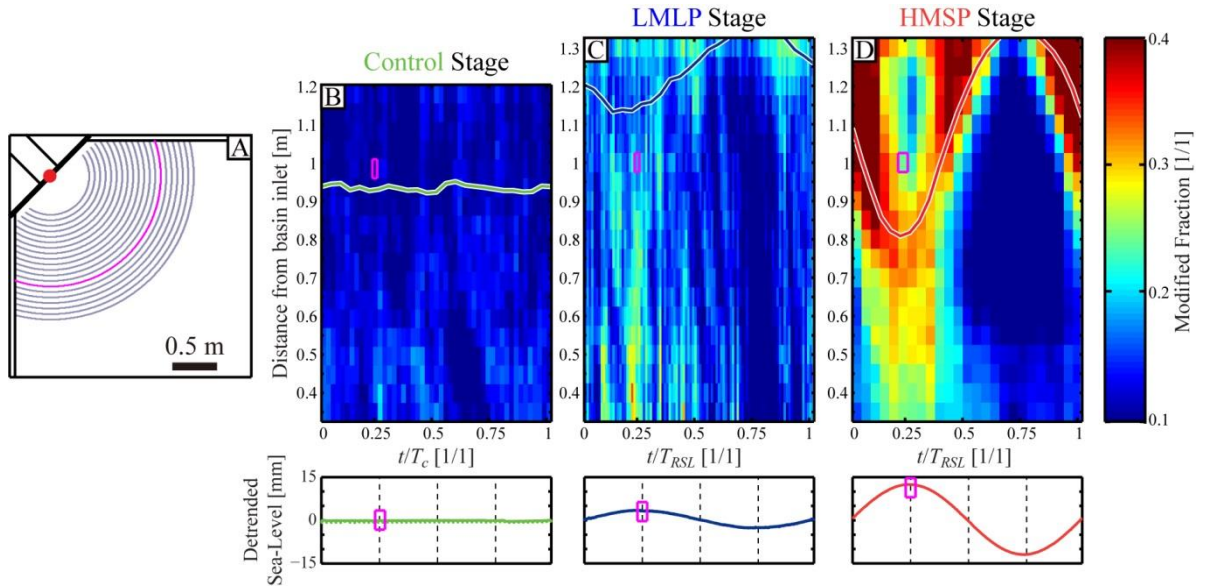


Figure 8: Data defining how the average fraction of a geomorphic surface modified by erosion or deposition over the course of a run-hour varies from proximal to distal basin locations and as a function of temporal position into a RSL cycle. A) Schematic of delta basin illustrating location of 20 transects used in analysis of surface modification fraction. B-D) Time-space maps of surface modification fraction for the control, LMLP, and HMSP stages, respectively. Below each time-space map a plot of detrended measured sea level is provided for reference. Solid lines within each time-space map indicate the average location of the shoreline. Magenta highlighted transect in basin schematic, outlined time-space map cells, and highlighted detrended sea level at $\frac{1}{4}$ way into RSL cycle illustrate how cells in the time-space maps are linked to distance from basin inlet, time into a RSL cycle, and associated value of detrended sea level.

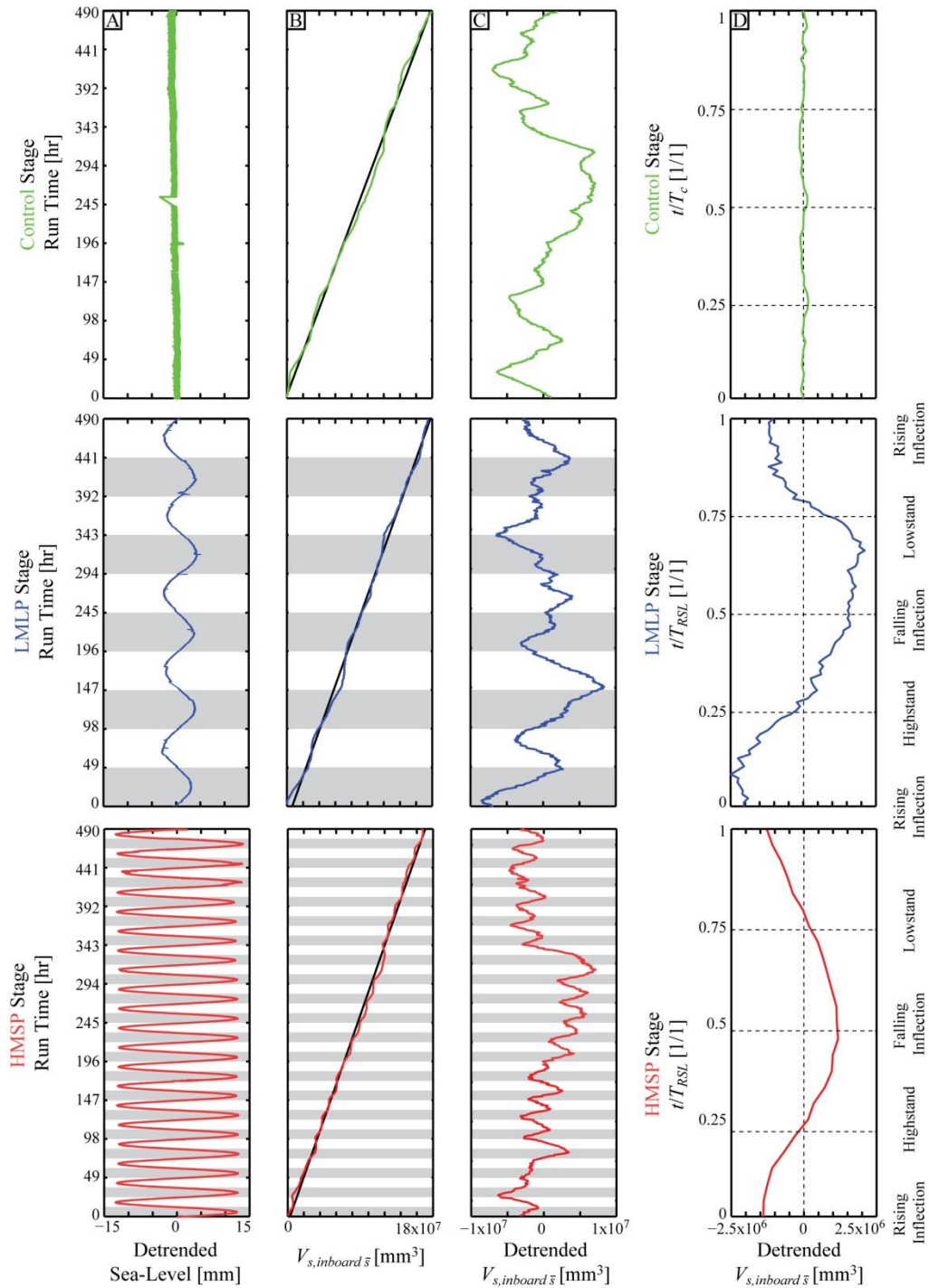


Figure 9: Data defining the measured response of deposit volume inboard of the average shoreline to changes in RSL. A) Time series of measured sea level detrended for long-term sea level rise in each experimental stage. B) Time series of the growth of the deposit volume inboard of the mean shoreline for each hour. Solid black line represents long term trend. C) Time series of the detrended deposit volume inboard of the mean shoreline. Gray bars indicate periods when sea level was higher than average. D) Average measured detrended deposit volume inboard of the mean shoreline for an RSL cycle.

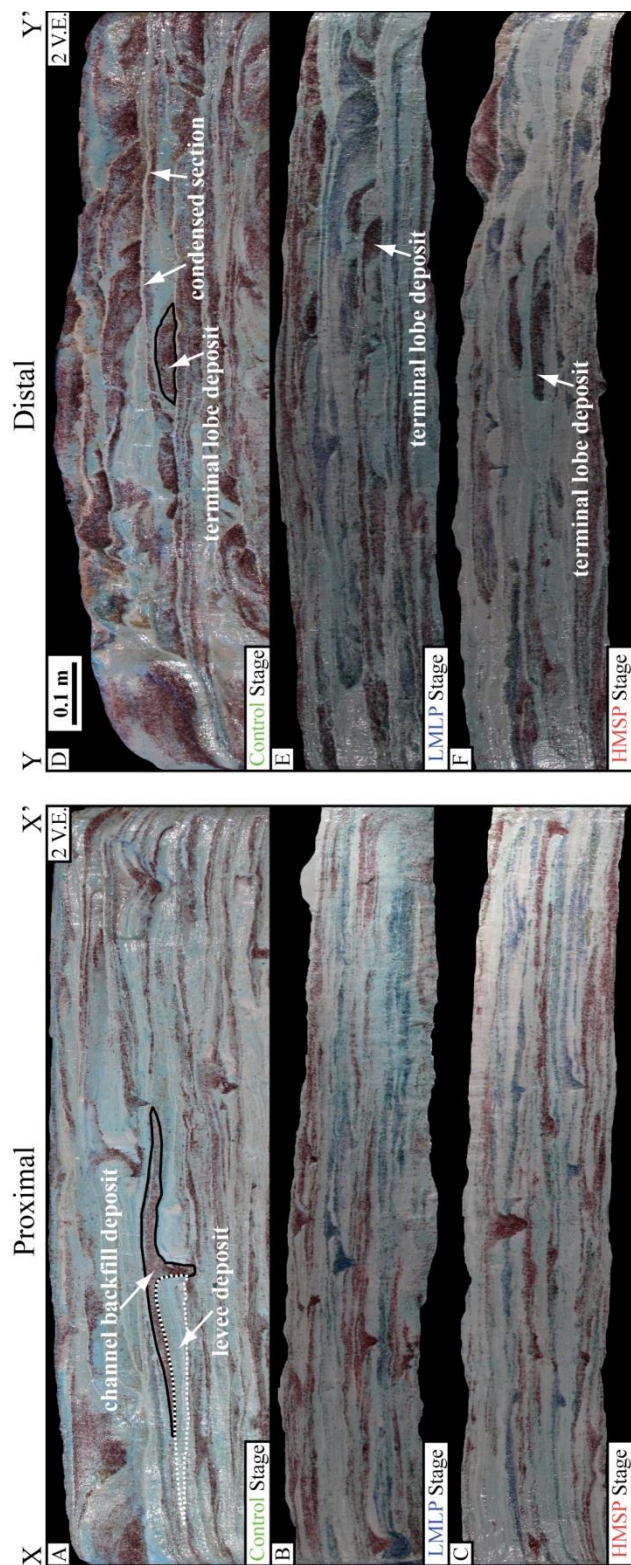


Figure 10: Images of preserved physical stratigraphy of the three experimental stages from proximal (A-C) and distal (D-F) strike oriented transects. Panels are oriented as if one were looking downstream and displayed with a vertical exaggeration of 2. Location of transects are shown in figure 1B.

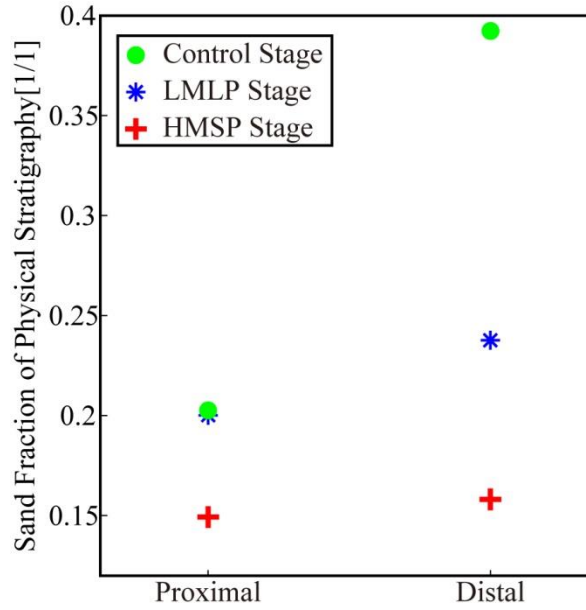


Figure 11: Colored sand as a fraction of total stratigraphic section measured from images of physical stratigraphy presented in figure 10.

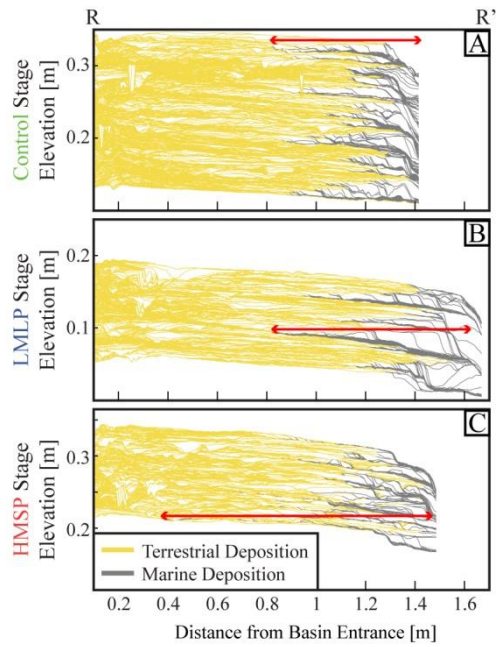


Figure 12: Panels of synthetic stratigraphy for a dip transect originating at the basin inlet. A-C) Preserved time-lines of the synthetic stratigraphy from the three experimental stages colored by environment of deposition. Red arrows show maximum lateral extent of parasequences in each stage. Location of transect shown in figure 13.

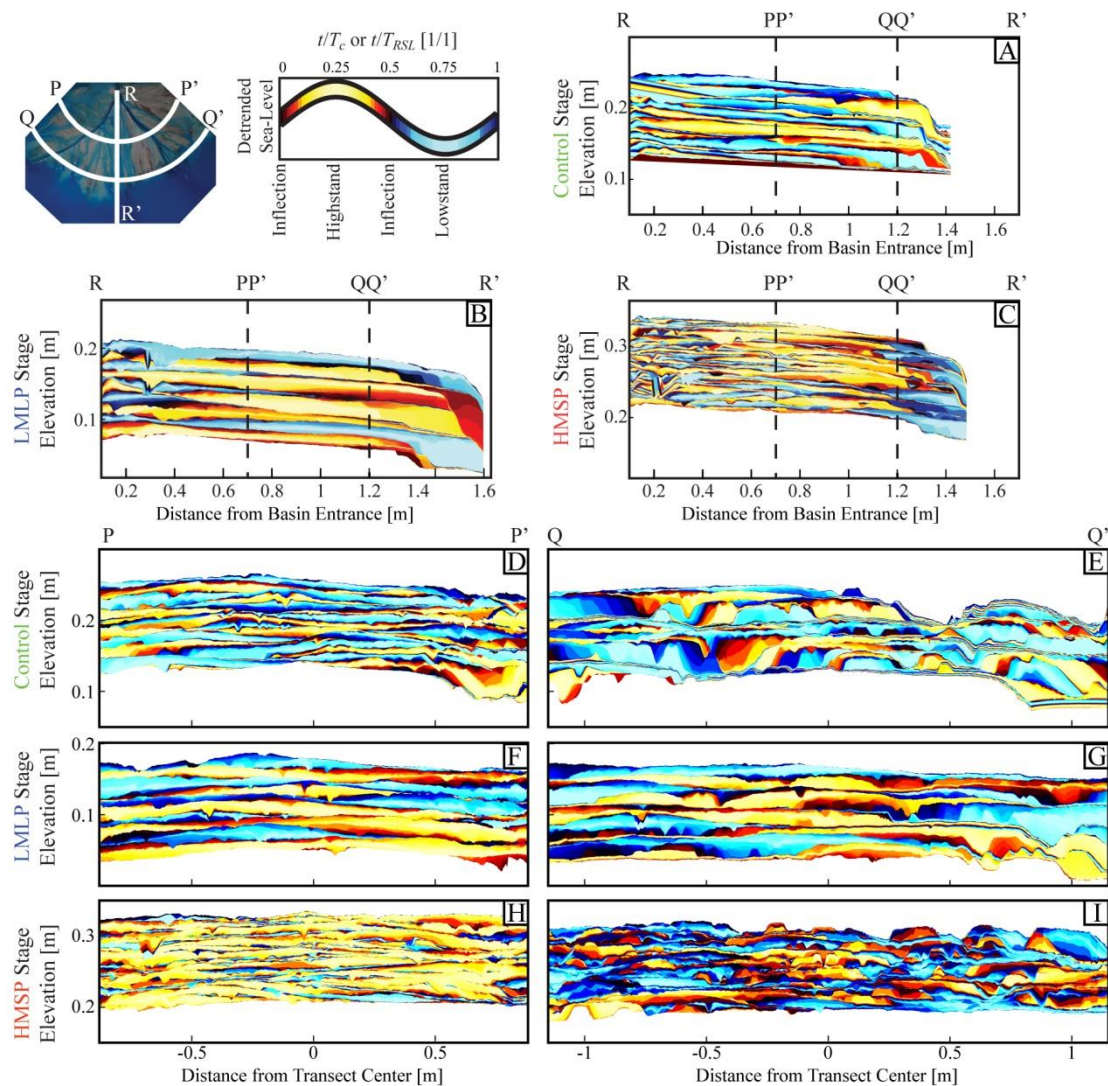


Figure 13: Panels of synthetic stratigraphy with deposits painted as a function of time of deposition within a cycle of RSL. Image at top-left details location of each transect while color bar details how synthetic stratigraphic color corresponds to time of deposition. Panels include a dip transect (A-C), and proximal (D, F, H) and distal (E, G, I) strike transects.

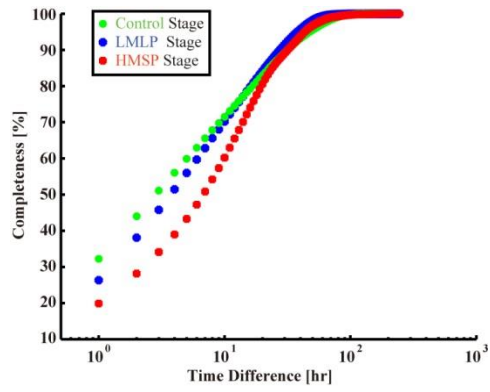


Figure 14: Stratigraphic completeness vs. time scale of discretization for the three experimental stages, measured from synthetic stratigraphy.

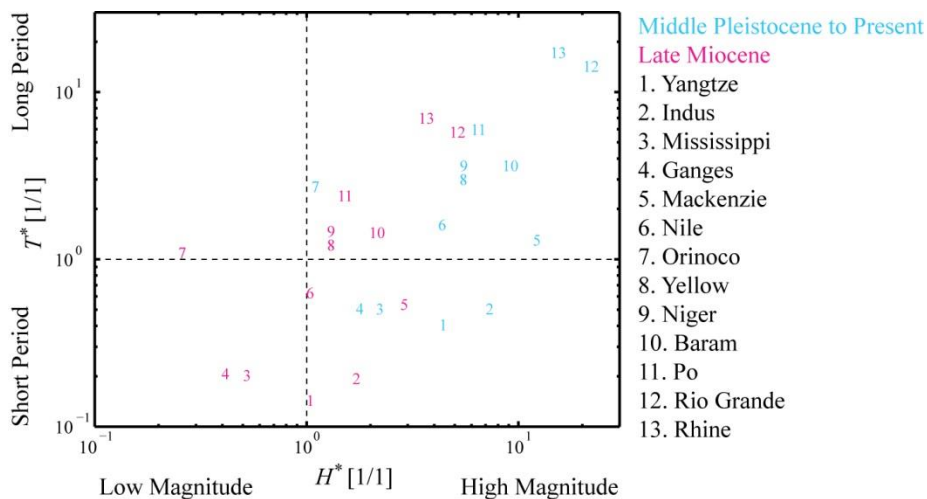


Figure 15: Predictions of magnitude and period of RSL cycles when normalized by autogenic length and time scales for 13 major river systems. Data originally published by Li et al. (2016). Predictions are for two time periods, the Middle Pleistocene to present (cyan) and the late Miocene (magenta) and are based on modern channel depths and long term (time window of measurement > 100 kyrs) sedimentation rates.

REFERENCES

- Ager, D. V., 1973, *The Nature of the Stratigraphic Record*, Wiley, 114 p.:
- Anderson, J. B., 2004, Late Quaternary stratigraphic evolution of the northern Gulf of Mexico margin: a synthesis, *in* Anderson, J. B., and Fillon, R. H., eds., *SEPM Special Publication No. 79*, p. 1-23.
- Barrell, J., 1917, Rhythms and the measurements of geologic time: *Geological Society of America Bulletin*, v. 28, no. 1, p. 745-904.
- Bhattacharya, J. P., 2011, Practical problems in the application of the sequence stratigraphic method and key surfaces: integrating observations from ancient fluvial-deltaic wedges with Quaternary and modelling studies: *Sedimentology*, v. 58, no. 1, p. 120-169.
- Blum, M. D., and Tornqvist, T. E., 2000, Fluvial responses to climate and sea-level change: a review and look forward: *Sedimentology*, v. 47, p. 2-48.
- Burgess, P. M., and Prince, G. D., 2015, Non-unique stratal geometries: implications for sequence stratigraphic interpretations: *Basin Research*, v. 27, no. 3, p. 351-365.
- Catuneanu, O., 2002, Sequence stratigraphy of clastic systems: concepts, merits, and pitfalls: *Journal of African Earth Sciences*, v. 35, no. 1, p. 1-43.
- Cazanacli, D., Paola, C., and Parker, G., 2002, Experimental steep, braided flow: application to flooding risk on fans: *Journal of Hydraulic Engineering*, v. 128, p. 322-330.
- Chamberlin, E. P., and Hajek, E. A., 2015, Interpreting paleo-avulsion dynamics from multistory sand bodies: *Journal of Sedimentary Research*, v. 85, no. 2, p. 82-94.
- Chow, V. T., 1959, *Open-channel hydraulics*, New York, McGraw-Hill, 680 p.:
- Csato, I., Catuneanu, O., and Granjeon, D., 2014, Millennial-Scale sequence stratigraphy: numerical simulation with Dionisos: *Journal of Sedimentary Research*, v. 84, no. 5, p. 394-406.
- Dalman, R., Weltje, G. J., and Karamitopoulos, P., 2015, High-resolution sequence stratigraphy of fluvio-deltaic systems: Prospects of system-wide chronostratigraphic correlation: *Earth and Planetary Science Letters*, v. 412, p. 10-17.
- Dorsey, R. J., Housen, B. A., Janecke, S. U., Fanning, C. M., and Spears, A. L., 2011, Stratigraphic record of basin development within the San Andreas fault system: Late Cenozoic Fish Creek–Vallecito basin, southern California: *Geological Society of America Bulletin*, v. 123, no. 5-6, p. 771-793.
- Famubode, O. A., and Bhattacharya, J. P., 2016, Sequence Stratigraphic Analysis of the Youngest Nonmarine Sequence In the Cretaceous Ferron Notom Delta, South Central Utah, USA: *Journal of Sedimentary Research*, v. 86, no. 3, p. 168-198.
- Flemings, P. B., and Grotzinger, J. P., 1996, STRATA: Freeware for analyzing classic stratigraphic problems: *GSA Today*, v. 6, no. 12, p. 1-7.
- Gilbert, G. K., 1890, *Lake Bonneville*, U.S. Geol. Surv. Monogr. 1.
- Granjeon, D., 1999, Concepts and applications of a 3-D multiple lithology, diffusive model in stratigraphic modeling.

- Hajek, E. A., Heller, P. L., and Schur, E. L., 2012, Field test of autogenic control on alluvial stratigraphy (Ferris Formation, Upper Cretaceous-Paleogene, Wyoming): Geological Society of America Bulletin, v. 124, no. 11-12, p. 1898-1912.
- Haq, B. U., 2014, Cretaceous eustasy revisited: Global and Planetary Change, v. 113, p. 44-58.
- Heller, P. L., Paola, C., Hwang, I. G., John, B., and Steel, R., 2001, Geomorphology and sequence stratigraphy due to slow and rapid base-level changes in an experimental subsiding basin (XES 96-1): Aapg Bulletin, v. 85, no. 5, p. 817-838.
- Hickson, T. A., Sheets, B. A., Paola, C., and Kelberer, M., 2005, Experimental test of tectonic controls on three-dimensional alluvial facies architecture: Journal of Sedimentary Research, v. 75, no. 4, p. 710-722.
- Hofmann, M. H., Wroblewski, A., and Boyd, R., 2011, Mechanisms Controlling the Clustering of Fluvial Channels and the Compensational Stacking of Cluster Belts: Journal of Sedimentary Research, v. 81, no. 9-10, p. 670-685.
- Hoyal, D. C. J. D., and Sheets, B. A., 2009, Morphodynamic evolution of experimental cohesive deltas: Journal of Geophysical Research-Earth Surface, v. 114, p. F02009.
- Hunt, D., and Tucker, M. E., 1992, Stranded parasequences and the forced regressive wedge systems tract: deposition during base-level fall: Sedimentary Geology, v. 81, no. 1-2, p. 1-9.
- Karamitopoulos, P., Weltje, G. J., and Dalman, R., 2014, Allogenic controls on autogenic variability in fluvio-deltaic systems: inferences from analysis of synthetic stratigraphy: Basin Research, v. 26, no. 6, p. 767-779.
- Karsenberg, D., and Bridge, J. S., 2008, A three-dimensional numerical model of sediment transport, erosion and deposition within a network of channel belts, floodplain and hill slope: extrinsic and intrinsic controls on floodplain dynamics and alluvial architecture: Sedimentology, v. 55, no. 6, p. 1717-1745.
- Kim, W., and Paola, C., 2007, Long-period cyclic sedimentation with constant tectonic forcing in an experimental relay ramp: Geology, v. 35, no. 4, p. 331-334.
- Kim, W., Paola, C., Swenson, J. B., and Voller, V. R., 2006, Shoreline response to autogenic processes of sediment storage and release in the fluvial system: Journal of Geophysical Research-Earth Surface, v. 111, no. F4, p. -.
- Kim, W., Sheets, B., and Paola, C., 2010, Steering of experimental channels by lateral basin tilting: Basin Research, v. 22, no. 3, p. 286-301.
- Koss, J. E., Ethridge, F. G., and Schumm, S. A., 1994, An Experimental-Study of the Effects of Base-Level Change on Fluvial, Coastal-Plain and Shelf Systems: Journal of Sedimentary Research Section B-Stratigraphy and Global Studies, v. 64, no. 2, p. 90-98.
- Li, Q., Yu, L. Z., and Straub, K. M., 2016, Storage thresholds for relative sea-level signals in the stratigraphic record: Geology, v. 44, no. 3, p. 179-182.
- Liang, M., Van Dyk, C., and Passalacqua, P., 2016, Quantifying the patterns and dynamics of river deltas under conditions of steady forcing and relative sea level rise: Journal of Geophysical Research: Earth Surface.

- Lynds, R. M., Mohrig, D., Hajek, E. A., and Heller, P. L., 2014, Paleoslope reconstruction in sandy suspended-load-dominant rivers: *Journal of Sedimentary Research*, v. 84, no. 10, p. 825-836.
- Martin, J., Cantelli, A., Paola, C., Blum, M., and Wolinsky, M., 2011, Quantitative Modeling of the Evolution and Geometry of Incised Valleys: *Journal of Sedimentary Research*, v. 81, no. 1-2, p. 64-79.
- Martin, J., Paola, C., Abreu, V., Neal, J., and Sheets, B., 2009, Sequence stratigraphy of experimental strata under known conditions of differential subsidence and variable base level: *AAPG Bulletin*, v. 93, no. 4, p. 503-533.
- Miller, K. G., Kominz, M. A., Browning, J. V., Wright, J. D., Mountain, G. S., Katz, M. E., Sugarman, P. J., Cramer, B. S., Christie-Blick, N., and Pekar, S. F., 2005, The phanerozoic record of global sea-level change: *Science*, v. 310, no. 5752, p. 1293-1298.
- Mohrig, D., Heller, P. L., Paola, C., and Lyons, W. J., 2000, Interpreting avulsion process from ancient alluvial sequences: Guadalupe-Matarranya (northern Spain) and Wasatch Formation (western Colorado): *GSA Bulletin*, v. 112, p. 1787-1803.
- Paola, C., and Borgman, L., 1991, Reconstructing random topography from preserved stratification: *Sedimentology*, v. 38, p. 553-565.
- Paola, C., Heller, P. L., and Angevine, C. L., 1992, The large-scale dynamics of grain-size variation in alluvial basins, 1: Theory: *Basin Research*, v. 4, p. 73-90.
- Paola, C., Straub, K. M., Mohrig, D., and Reinhardt, L., 2009, The "unreasonable effectiveness" of stratigraphic and geomorphic experiments: *Earth -Science Reviews*, v. 97, p. 1-43.
- Plint, A. G., 2009, High-frequency Relative Sea-level Oscillations in Upper Cretaceous Shelf Clastics of the Alberta Foreland Basin: Possible Evidence for a Glacio-Eustatic Control? *Sedimentation, Tectonics and Eustasy: Sedimentation, Tectonics and Eustasy, Spec. Publ. Int. Assoc. Sedimentol*, v. 12, p. 409-428.
- Sadler, P. M., and Strauss, D. J., 1990, Estimation of Completeness of Stratigraphical Sections Using Empirical Data and Theoretical-Models: *Journal of the Geological Society*, v. 147, p. 471-485.
- Stanley, D. J., Warne, A. G., and Dunbar, J. B., 1996, Eastern Mississippi delta: late Wisconsin unconformity, overlying transgressive facies, sea level and subsidence: *Engineering Geology*, v. 45, no. 1, p. 359-381.
- Straub, K. M., and Esposito, C. R., 2013, Influence of water and sediment supply on the stratigraphic record of alluvial fans and deltas: Process controls on stratigraphic completeness: *Journal of Geophysical Research - Earth Surface*, v. 118, p. 13.
- Straub, K. M., Li, Q., and Benson, W. M., 2015, Influence of sediment cohesion on deltaic shoreline dynamics and bulk sediment retention: A laboratory study: *Geophysical Research Letters*, v. 42, no. 22, p. 9808-9815.
- Vail, P. R., Mitchum, R. M., and Thompson, S., 1977, Seismic stratigraphy and global changes of sea level, Part 4: Global cycles of relative changes of sea level, *in* Payton, C. E., ed., *AAPG Memoir 26 Seismic Stratigraphy - Applications to Hydrocarbon Exploration*, p. 83-98.

- Van Dijk, M., Postma, G., and Kleinhans, M. G., 2009, Autocyclic behaviour of fan deltas: an analogue experimental study: *Sedimentology*, v. 56, no. 5, p. 1569-1589.
- Van Heijst, M. W. I. M., and Postma, G., 2001, Fluvial response to sea-level changes: a quantitative analogue, experimental approach: *Basin Research*, v. 13, p. 269-292.
- Van Wagoner, J. C., 1995, Sequence stratigraphy and marine to nonmarine facies architecture of foreland basin strata, Book Cliffs, Utah, U.S.A., *in* Van Wagoner, J. C., and Bertram, G. T., eds., *Sequence Stratigraphy of Foreland Basin Deposits: Outcrop and Subsurface Examples from the Cretaceous of North America*, Volume 64, American Association of Petroleum Geologists, Memoirs, p. 137-223.
- Van Wagoner, J. C., Mitchum, R. M., Campion, K. M., and Rahmanian, V. D., 1990, Siliciclastic sequence stratigraphy in well logs, cores, and outcrops: Concepts for high-resolution correlation of time and Facies: *AAPG Methods in Exploration* 7, 55 p.:
- Wang, Y., Straub, K. M., and Hajek, E. A., 2011, Scale-dependent compensational stacking: An estimate of autogenic time scales in channelized sedimentary deposits: *Geology*, v. 39, no. 9, p. 811-814.
- Wheeler, H. E., 1964, Baselevel, lithosphere surface, and time-stratigraphy: *Geological Society of America Bulletin*, v. 75, no. 7, p. 599-610.
- Wood, L. J., Ethridge, F. G., and Schumm, S. A., 1993, The effects of rate of base-level fluctuation on coastal-plain, shelf and slope depositional systems; an experimental approach, *in* Posamentier, H. W., Summerhayes, C. P., Haq, B. U., and Allen, G. P., eds., *Sequence Stratigraphy and Facies Associations*. Special Publication of the International Association of Sedimentologists, p. 43-53.

BIOGRAPHY

After completion of high school in China in the year 2010, Lizhu Yu went to U.S. and enroll in the University of Wyoming. She received her Bachelor of Science degree in geology in 2014. Afterwards, Lizhu went to Tulane University to pursue her Master's degree in geology. She worked with Professor Kyle Straub in Tulane's Sediment Dynamics Laboratory and conducted a suite of physical experiments to quantitatively analyze the stratigraphic characteristics. Upon graduation Lizhu plans to move to California and explore work opportunities in energy industry.